A Proposed Methodology for Reconciling High-Resolution Numerical Modeling Guidance with Pattern Recognition to Predict Lake-Effect Snow

MICHAEL EVANS and RON MURPHY

NOAA/National Weather Service, Binghamton, NY

(Submitted 5 October 2007; in final form 11 March 2008)

ABSTRACT

Current methodologies for using numerical guidance to help with the forecasting of lake effect snow typically involve either 1) examination of numerical models with horizontal grid spacing small enough to explicitly forecast the structures associated with lake effect snow bands, or 2) examination of numerical models with relatively large horizontal grid spacing to forecast the meso-scale flow pattern, then application of experience or pattern recognition to predict the location, structure and intensity of the resultant snow bands. This paper demonstrates an application developed at the National Weather Service Forecast Office in Binghamton, New York, that aids forecasters with the pattern recognition aspect of lake effect snow forecasting. A forecasting process that combines pattern recognition with explicit output from a model with small horizontal grid spacing is demonstrated through examination of two case studies. Results from the case studies show that the pattern recognition application can be used to provide forecasters with useful information on the range of possible outcomes that could occur with a given meso-scale flow pattern. In addition, the case studies indicate that comparing forecasts from high-resolution models with output from the pattern recognition application can provide forecasters with increased confidence in the numerical guidance in some cases, and can help forecasters to improve on the numerical guidance in other cases.

---

1. Introduction

Lake-effect snow develops downwind of the Great Lakes in response to polar, continental or arctic air masses crossing the relatively warm waters of the lakes. A temperature difference

Corresponding author address: Michael Evans, National Weather Service, 32 Dawes Drive, Johnson City, NY 13790. E-mail: Michael.evans@noaa.gov

(ΔT) of 13 ºC between the lake and 850 hPa has long been used as a minimum operational threshold for the development of lake-effect snow in the absence of synoptic-scale forcing (Rothrock 1960). Air masses associated with lake-effect snow are typically characterized by mid-tropospheric subsidence. As a result, the atmospheric wind and temperature profile associated with lake-effect snow outbreaks typically feature a surface-based mixed layer associated with strong vertical moisture and heat fluxes from the underlying lake surface, capped by a subsidence inversion. Favorable factors for intense, well-organized outbreaks of lake-effect snow include a deep surface-based mixed layer (Byrd et al. 1991), with small directional wind shear (Niziol et al. 1995). Orographic lift downstream of the lakes can also play a major role in intensifying lake-effect snows (Reinking et al. 1991). Finally, in some cases, snowfall associated with large-scale lifting can be enhanced when the large-scale lifting becomes superimposed on an environment characterized by cold air over a warm lake with a ΔT less than 13 ºC ("lake-enhanced" snowfall, Dockus 1985, Lackman 2001).

An idealized modeling study by Laird et al. (2003) indicated that large, single bands of lake-effect snow are favored downwind of elongated lakes in environments where the wind has a long over-water fetch, and the resultant over-water fetch to wind speed ratio is large. A more widespread coverage of narrow bands (multi-bands) is favored when the over-water fetch and resultant fetch to wind speed ratio decreases. This has also been shown observationally (Niziol et al. 1995). In central New York, operational experience indicates that boundary layer flows with a direction from 250º to 300º, roughly parallel to the long axis of Lake Ontario, are associated with long enough over-water fetch lengths to produce large, single bands of heavy snow over and downwind of the lake. Meanwhile, directions of greater than 300º typically reduce the over-

water fetch sufficiently to produce widespread finer-scale multi-bands of lake-effect snow southeast or south of Lake Ontario.

Previous modeling studies have indicated that models with sufficiently small horizontal grid spacing can produce realistic simulations of large, single bands of lake-effect snow. For example, Ballentine et al. (1998) documented a simulation of a 15 km wide, intense west-east oriented single band of heavy snow over and downwind of Lake Ontario. The model used in the simulation had a 5 km horizontal grid spacing over eastern and central Lake Ontario, nested within a 15 km grid covering the entire area from Lake Huron through upstate New York. Precipitation distribution and amounts in the simulation matched well with observations during the first 12 hours of the simulation. Niziol (2003) documented a successful simulation of a band with similar dimensions east of Lake Erie, using an 8 km model. Smaller bands can also be simulated, however even smaller horizontal grid spacing is required. For example, Watson et al. (1998) successfully simulated smaller north-south oriented snow bands (widths approximately 5 km) south of the Finger Lakes in central New York, using a nested model with a 2.5 km inner nest centered over the Finger Lakes.

The current suite of National Oceanic and Atmospheric Administration (NOAA) National Center for Environmental Prediction (NCEP) operational forecast models are characterized by horizontal grid spacing near or slightly greater than what has been shown to produce realistic simulations of large lake-effect snow bands in the aforementioned studies, and are much too large to simulate smaller bands [the current horizontal grid spacing is 12 km for the North American Meso-scale (NAM) model (Rogers et al. 2001), and 13 km for the operational Rapid

Update Cycle (RUC) model, (Benjamin et.al. 2004)]. Operational experience indicates that these models often produce realistic simulations of large single band snow events, although the intensity of the bands (based on quantitative precipitation forecasts (QPFs)) are typically under-forecast. Experience also shows that these models do not explicitly simulate the finer-scale reflectivity patterns that are typically observed in more widespread multi-band lake-effect snow events.

Given the resolution limitations of current operational models, forecasters making explicit forecasts of small-scale multi-bands of lake-effect snow are left with two options. The first option is to examine a local model with small enough horizontal grid spacing to explicitly simulate the smaller structures. One problem with this approach is that computing power typically available in an operational environment limits local models to grid spacing of 5 to 10 km, which represents a decrease in grid spacing compared to the NCEP operational models, but is still insufficient to fully simulate fine-scale bands. In addition, it has been shown that simply decreasing the horizontal grid spacing of a model does not automatically improve QPFs in a convective regime (Gallus 1999). The second approach is to use a model with larger horizontal grid spacing to forecast the meso-scale environment, then use experience and "rules of thumb" to deduce the structure, intensity and expected location of small-scale lake-effect snow bands. At our current stage, most forecasters combine pattern recognition from meso-scale patterns forecast by NCEP operational models with explicit output from models with larger horizontal grid spacing that may still not fully capture the smaller-scale bands. Forecasters typically finalize their forecasts by attempting to blend information from both approaches.

This paper consists of two case studies that will demonstrate how both approaches can be used, and how the results from both approaches can be blended to make forecasts for lake-effect snow. To demonstrate the utility of a model with small horizontal grid spacing, output will be shown from a 6-km implementation of the Weather Research and Forecasting (WRF) model (Zavisa, 2004). While this horizontal grid spacing is still not sufficient to explicitly simulate narrow multi-bands of lake-effect snow, it will be shown that this resolution is adequate to produce structures that are significantly more detailed than what is produced by the 12 km NAM. More details on the configuration of this model are given in section 2. Regarding the use of models with larger horizontal grid spacing and the subsequent application of pattern recognition, this paper will detail the use of an application developed at the National Weather Service Forecast Office (WFO) in Binghamton, NY (BGM) which aids forecasters by allowing them to compare output from real time NCEP models to data from a large database of historical lake-effect snow events. More details on this application are presented in section 2. Section 3 of this paper consists of the two case studies, and section 4 contains a summary and conclusion.

2. Methodology

Forecasts from models with small horizontal grid spacing shown in this paper are from a workstation version of the WRF model, using the Non-hydrostatic Mesoscale Model (NMM) dynamic core, run at the NWS forecast office in Buffalo, NY (BUF). The model was run with a 6 km horizontal grid spacing and 45 vertical levels over a domain covering the eastern and central Great Lakes area eastward through most of upstate New York (Fig. 1). The initial and boundary conditions for the model are provided by 12 km NAM grid tiles (the AWIPS 218 grid)

at 6 hour temporal resolution. As such, an accurate depiction of air mass modification over the upwind western Great Lakes (i.e., Lakes Michigan and Superior) is dependent on the NAM forecast. (Sousounis and Mann (2000) have described the critical role that upstream lakes can play in the evolution of lake effect snow). The model is run with explicit convection, the new Ferrier microphysics scheme (Ferrier et. al. 2002), and the Mellor-Yamada-Janjic boundary layer scheme (Janjic 1996). Although 6 km is near the threshold of recommended use of explicit convection (i.e., Weisman et al. 1997), the shallow nature of the convective motions associated with lake-effect snow do not typically trigger deep convection in traditional convective parameterizations, thus explicit convection was used.

The pattern recognition application tool developed at BGM [available online at: http://www.lightecho.net/les/] works by comparing NAM model forecast sounding data to data in a historical database of NAM forecast sounding parameters. The database contains parameters from 6-hour NAM forecast soundings from over 300 cases that occurred from 2003-2007. Data were collected at times when lake-effect snow was occurring somewhere across central New York, or when the flow across the area had a trajectory that originated over the Great Lakes in combination with air temperatures that were low enough to potentially support lake-effect snow (based on a ΔT of at least 13 ºC.), yet no snow occurred (null events). At each time, BUFKIT visualization software (Mahoney and Niziol 1997; http://www.wbuf.noaa.gov/bufkit/bufkit.html) was used to collect 6-hour forecast data at 3 points located downstream from Lake Ontario: Syracuse, NY (SYR), Ithaca, NY (ITH) and Binghamton, NY (BGM). Forecasters use the application by examining current model forecast output at one of these forecast points, then entering several, key corresponding forecast sounding parameters into a table. The application

then performs a search of the historical database, and returns a list of the 5 historical events that are most similar to the current event, based on similarity of the sounding parameters. Note that the analogue cases are matched on a 6-h time resolution, therefore a historical match for a current case at 0600 UTC may or may not be the same match returned for the same case at 0000 UTC. Finally, the application provides forecasters access to web pages that contain information on these "most similar" events, including radar images, forecast soundings and text descriptions (including snowfall amounts). Forecasters can use this information to anticipate a range of possible evolutions for the current event. More details on the algorithm for determining the most similar, historical events are given in the appendix.

The key sounding parameters were chosen to best describe the attributes of a sounding that are most critical to the occurrence and evolution of lake effect snow, based on a review of previous research, plus local experience. The parameters are:

- the boundary-layer mean wind speed and direction (where the boundary layer is defined as the layer from the 3rd sigma layer of the model to the base of the subsidence inversion),
- the 850 hPa temperature,
- the ΔT between 850 hPa and Lake Ontario (based on lake temperature data from the Great Lakes Environmental Research Lab),
- the height of the base of the subsidence inversion (an algorithm for determining the base of the inversion is given in the appendix),
- the depth of the moist layer, as defined by all layers with a dew point depression of 3^{o} C or less,
- the maximum dew point depression below 900 hPa,

- the depth of the dendritic snow growth layer, defined as any moist layers where temperatures are between -12º and -18º C,
- the maximum upward vertical motion within the dendritic snow growth layer, and
- the root mean square (RMS) of the wind in the boundary layer.

A parameter for event duration is also included, where events associated with boundary layer wind directional variation of 10º or less over a period of 12 hours or more are designated as "persistent". Finally, time of day is considered, allowing for the fact that afternoon and early evening lake-effect snow is often more cellular than during the late night or early morning, when more organized banded structures typically occur (Kristovich and Spinar 2004).

3. Case Studies

a. 16-17 January, 2007

Lake-effect snow showers developed downwind of Lake Ontario across central New York during the morning on 16 January 2007, as a cold northwest flow developed over the lake. Figs. 2-4 show output from the NCEP NAM model run at 12 UTC on the 16th. Cold northwest flow is evident over and downwind of the Great Lakes (Fig. 2), indicating a condition that would be favorable for the development of multi-band lake-effect snow across central New York. The flow was forecast to veer slightly through the period, but no pronounced wind shifts were indicated. Little organized upward vertical motion was indicated across central New York at 18 UTC (Fig. 3a), then a weak plume of upward vertical motion was forecast to develop downwind of Lake Ontario from 00 UTC through 06 UTC (Figs. 3b-c). The upward motion diminished by

12 UTC (Fig. 3d). In this case, the 12 km NAM only forecast a small area of very light precipitation between BGM and SYR during the period ending at 06 UTC (Fig. 4c), with no precipitation at any of the other time periods (Figs. 4a,b and d).

Forecast output from the 6 km workstation WRF run at BUF, is shown in Figs. 5a-d. Unlike the 12 km NAM, the 6 km WRF was able to explicitly forecast precipitation across much of central New York, at several different time periods between 12 UTC 16 January and 12 UTC 17 January . The implied precipitation was very light and disorganized through 00 UTC (Figs 5a, b), then organized into a distinct northwest-southeast oriented band just south of SYR by 06 UTC (Fig. 5c). The band shifted south toward BGM by 12 UTC (Fig. 5d). The total QPF from this model run through 12 UTC 17 January is shown in Fig. 6. Much of the area between SYR and BGM was forecast to receive some precipitation, with a maximum between 0.10 and 0.13 inches southwest of SYR.

Based on the model forecast data shown so far, a forecaster making a prediction during the morning on 16 January would expect some accumulating lake-effect snow between 12 UTC 16 January and 12 UTC 17 January,' across the area from SYR south to BGM. The fact that both the 12 km NAM and 6 km WRF indicated that the maxima of precipitation would occur just south of SYR would give the forecaster increased confidence of that location. However, the fact that the two models forecast significantly different amounts (a maximum of 0.03 inches for the 12 km NAM vs. a maximum of 0.13 inches for the 6 km WRF) would introduce uncertainty. At this point, it might be helpful to compare this event with some previous, similar events in order

to 1) increase the forecaster's confidence on the expected location of heaviest snow, and 2) to give the forecaster some insight on how much snow similar events have historically produced.

Figs. 7a-d show forecast soundings from the NAM at SYR, valid on 16-17 January 2007 and displayed by BUFKIT visualization software. The display shows model forecast temperature, dew point and wind profiles on the right, and a map of the forecast area on the left, including a box outlining the most likely location for lake-effect snow based on the boundary layer mean wind direction and climatological studies done at BUF (Kolker 1978). The color of the box is dependent on the amount of wind shear in a user-defined boundary layer, with green indicating small shear, yellow indicating moderate shear, and red indicating large shear (Mahoney and Niziol 1997). Figs. 8a-d show output from the pattern recognition application, after forecast data from the 12 UTC NAM was entered, and the database search was executed. The left columns in each table contain sounding parameter values from each time for the current event, and the remaining columns contain data from the corresponding, historical, most similar events.

The data shown in Figs. 7 and 8 depict an event characterized by several hours of weakly sheared northwesterly flow. The base of the inversion was forecast around 800 hPa near the start of the event, lowering slightly by the end of the event. Moist layers were forecast to be quite shallow, and constrained to levels below the base of the subsidence inversion. Note that this event was characterized as "non persistent" at 18 UTC, and 12 UTC, but "persistent" at 00 UTC and 06 UTC. Recall that "persistent" events are defined as events with a boundary layer wind directional variation of 10^{o} or less for a period of 12 hours or more. When an event is

characterized as “persistent”, the corresponding similar events are also more likely to be “persistent” and therefore are more likely to be associated with larger event total snowfalls.

Comparisons between 0.5º radar reflectivity imagery from the Binghamton WSR-88D Doppler radar (KBGM) at 18 UTC 16 January, and corresponding imagery from the top 3 “most similar” historical dates and times are shown in Fig. 9. The observed 0.5º reflectivity pattern at 18 UTC was characterized by a cellular snow shower pattern, with weak embedded banding across central New York (Fig. 9a). Radar imagery from the 3 most similar events (Figs. 9b-d) all indicated broken bands of light snow showers across the area from SYR south to BGM. Text summaries from these historical cases (available via the application, not shown), indicate that all 3 of these events produced only light snow showers between SYR and BGM, with no significant accumulations around the time that the imagery is shown.

Fig. 10a shows that the snowfall pattern at 00 UTC 17 January evolved into several, narrow northwest-southeast oriented snow bands between SYR and BGM. The most similar event was characterized by several northwest-southeast oriented bands across central NY and northeast Pa, with most of the coverage centered over the SYR area (Fig. 10b). The text summary for this historical event indicated that the snow bands in the SYR area persisted for nearly 48 hours, which resulted in heavy snow accumulations (greater than 10 inches). This result highlights a caveat when using this application for anticipating snow amounts. While both the current and historical event in this case were classified as “persistent”, the current event was persistent for only about 12 hours, while the historical event was persistent for about 48 hours. As a result, the historical event may have been a good analogue for anticipating a “snap-shot” of

the snow banding structure, but it was not a good analogue for anticipating event total snowfall. The 2nd event (Fig. 10c) was characterized by weak, broad bands of light snow across central New York. Only light snow accumulations were occurring during the time of the image. The 3rd event was associated with several narrow, northwest to southeast oriented bands, mainly along and east of a line from SYR to BGM (Fig. 10d). The text discussion for this case indicated that these snow bands were associated with accumulations of 2 to 4 inches.

The snowfall pattern at 06 UTC 17 January was characterized by a single, narrow, northwest to southeast oriented band of snow near BGM, surrounded by weaker bands (Fig. 11a). The radar imagery from similar event # 1 indicated some narrow, broken bands in the SYR area (Fig. 11b). The text summary for this case indicated that the SYR area picked up from 2 to 5 inches of snow from this event, with less to the south. The second and 3rd events were associated with radar imagery that appeared to be quite similar to what was observed; namely several northwest to southeast oriented bands centered near BGM (Figs. 11c-d). The text summaries from both cases indicated that none of these bands produced more than 4 inches of snow in a 12 hour period. Fig. 12a shows that little if any snow was falling at 12 UTC 17 January. The radar imagery from similar event # 1 also indicated no snow (Fig. 12b). Events 2 and 3 were associated with weak multi-bands, producing little if any accumulation (Figs 12c-d).

In summary, the radar reflectivity patterns during this event transitioned from a cellular pattern of snow showers with weak embedded bands during the afternoon on 16 January, to weak-to-moderate, narrow northwest-southeast oriented bands from SYR south to near BGM during the evening through early morning hours on 17 January, to nothing by 12 UTC 17

January. The pattern recognition application shown in this paper returned events that would have given the forecaster strong indications for that type of evolution. Except for 1 event that persisted for nearly 48 hours, the historical event text summaries indicated that snowfall associated with the multi-bands were light (less than 5 inches in 12 hours). These types of accumulations would give a forecaster reasonable confidence in the liquid precipitation amounts of 0.01 to 0.13 inches forecast by the 6 km WRF, given that snow to liquid ratios for lake-effect snow events that are this cold are typically 20 to 1 or more (based on operational experience). The pattern recognition application in this case confirmed the high resolution numerical guidance that a small accumulation of snow could be expected between SYR and BGM through 12 UTC 17 January. Fig. 13 shows the observed snowfall from 12 UTC 16 January through 12 UTC 17 January. Snowfall occurred throughout the area between BGM and SYR, with amounts generally ranging between 1 and 3 inches, and isolated totals of 5 inches.

b. 17-18 March, 2007

Another, more significant lake-effect snow event developed southeast of Lake Ontario on 17 March, 2007. A cold northwest flow was indicated through the period, similar to the previous case (c.f., Figs. 2 and 14). Unlike the previous case, the northwest flow was co-located with a deep layer of near saturation in the lower and mid-troposphere, in the wake of a major east-coast cyclone moving northeast toward the Canadian Maritimes (not shown). A disorganized pattern of upward vertical motion east-southeast of Lake Ontario at 18 UTC was forecast to evolve into a broad northwest to southeast oriented band of ascent across central New York by 00 UTC 18 March (Figs. 15a-b). The band was forecast to persist through 06 UTC, then pull northward and

weaken by 12 UTC (Figs. 15c-d). The resultant NAM QPF is shown in Figs. 16a-d. A broad area of light precipitation south of Lake Ontario was forecast through 00 UTC (Fig. 16a). The light precipitation expanded southeast toward northern Pennsylvania by 06 UTC, then diminished and pulled back to the north by 12 UTC (Fig 16b-c). The 24-hour QPF ending at 12 UTC 18 March indicated a large area of greater than 0.25 inches across central New York south of Lake Ontario, with a band of 0.10 inches extending south across portions of northeast Pennsylvania (Fig. 16d).

Figs. 17a-d show the same fields as Fig. 16, except that the data is from the 6 km WRF model. The same evolution indicated by the NAM was also indicated by the 6 km WRF. Specifically, a broad area of light precipitation south of Lake Ontario during the afternoon on 17 March (Fig. 17a) was forecast to evolve into an elongated band of precipitation extending southeast into northern Pennsylvania during the evening (Fig. 17b). The 24-hour QPF (Fig. 17d) indicated totals of greater than 0.5 inches across a broad area south of SYR, with a band of 0.1 to 0.25 inches extending southeast from near ITH west of BGM into northern Pennsylvania. Forecasters interpreting data from the NAM and 6 km WRF could conclude that a disorganized snow shower pattern during the afternoon on 17 March would evolve into a more organized pattern of significant northwest-southeast oriented snow bands during the evening hours. Several inches would be likely across the area just south of SYR, with a few inches likely in bands extending from ITH across the area west of BGM and into northern Pennsylvania. Lake-effect snow producing accumulations of several inches is a common occurrence in the SYR area, however lake-effect snow accumulations of more than 4 inches in 12 hours is rather uncommon across the southern tier of New York or northern Pennsylvania. With the NAM and the 6 km

WRF indicating the development of significant snow bands across that area, forecasters were looking at the possibility of a relatively unusual event. In these situations, application of pattern recognition can be useful to confirm and refine the model forecasts, or to call the forecasts into question.

Figs. 18a-d show model forecast soundings at ITH from the 12 km NAM, valid at 18 UTC 17 March, 00 UTC 18 March, 06 UTC 18 March, and 12 UTC 18 March. As in the first case, a persistent northwest flow was indicated through the period. In contrast to the first case, the soundings indicated a persistent, deep layer of near saturation in the lower to mid troposphere. A weak inversion, located at about 850 hPa at 18 UTC was shown to dissipate by 00 UTC. The mean wind in the deep, well-mixed boundary layer backed gradually from around 330º early in the event to around 315º by 12 UTC, while retaining a nearly unidirectional shear profile. Wind directions greater than about 320 º are favorable for enhancement of lake-effect snow bands downstream of the Finger Lakes over southern New York (Sobash et al. 2005). Figs. 19a-d show the sounding parameters from each time shown in Fig. 18, after the appropriate data was entered into the application, and the database search was executed. The left column in each figure contains the sounding parameters from the case being examined, and the remaining columns contain data from the corresponding historical "most similar" events.

Figs. 20a-d show comparisons between KBGM 0.5º radar reflectivity imagery at 18 UTC and corresponding imagery from the top 3 "most similar" historical dates and times. Fig. 20a shows that the pattern at 18 UTC indicated a large area of light snow across central New York, with some heavier embedded cellular features located mainly north and west of BGM. The most

similar event was characterized by a cellular pattern of snow showers, with accumulations of 2 to 3 inches across central New York north of BGM (Fig. 20b). The second event was characterized by a widespread area of light snow, with a few embedded snow bands extending from the Finger Lake area southeast toward northern Pennsylvania. The text summary for this event indicated that accumulations of 2 to 5 inches were widespread across central and southern New York. The third event also indicated a large area of light snow with a few embedded heavier snow showers near BGM southward across northern Pennsylvania. Snow accumulations with this event were less than one inch.

The 0.5º radar reflectivity at 00 UTC was characterized by a broad area of light snow across central New York, with a distinct band of heavier snow extending from the Finger Lakes near ITH southeast across south central New York (Fig. 21a). The most similar, historical event also showed a large area of light snow across central New York with an intense band extending from near ITH southeast across northeast Pennsylvania (Fig. 21b). Snowfall amounts with this most similar, historical event ranged from 2 to 6 inches across much of central New York and northern Pennsylvania, with a maximum of near 10 inches close to ITH. The second-most similar, historical event was also returned as a similar event to 18 UTC. Enhanced snow bands from the Finger Lakes near ITH can be seen extending southeast into northeast Pennsylvania, producing 2 to 5 inches of snow (Fig. 21c). The third most similar, historical event indicated a more disorganized, convective pattern, with some enhanced banding over central New York and northern Pennsylvania (Fig. 21d). Snow amounts during this period were 2 inches or less.

Fig. 22a shows that the 0.5º radar reflectivity at 06 UTC indicated a very intense snow band west of ITH, with other significant northwest-southeast bands located across central New York and northern Pennsylvania. The most similar, historical events all indicated significant snow bands extending from the Finger Lakes southeast toward northern Pennsylvania (Figs. 22b-d). The first two images were associated with 2 to 5 inch snow events for southern New York and northern Pennsylvania, and the next image was associated with the event that produced a widespread 2 to 6 inch snowfall across southern New York and northern Pennsylvania, with a maximum of 10 inches near ITH.

The 0.5º radar reflectivity at 12 UTC indicated a few narrow, moderately intense northwest to southeast snow bands persisting across central New York and northeast Pennsylvania (Fig. 23a). The bands had shifted northeast from their earlier position. The most similar, historical event returned by the application indicated a west-northwest to east-southeast oriented band located near BGM, surrounded by other, weaker bands (Fig. 23b). The text summary from this event indicated a 3 to 5 inch snowfall across the southern Finger Lakes area. The second historical event indicated a more widespread snow event than what was observed at 12 UTC, with snow amounts across the Finger Lakes and southern tier of New York ranging from 2 to 5 inches (Fig. 23c). The third event showed snow bands in a similar orientation as to what was observed at 12 UTC, however the bands were considerably weaker (Fig. 23d). All of the analog cases indicated that the bands would have an increasingly west-to-east orientation by 12 UTC, as opposed to the northwest-to-southeast orientation indicated earlier in the morning.

In summary, the pattern recognition application in this case correctly indicated that this would be an event characterized by significant snow bands extending from the Finger Lakes area near ITH southeast across northeast Pennsylvania. One of the similar events identified by the application was associated with a snowfall maximum of 10 inches near ITH, with most of the other events associated with amounts in the 2 to 5 inch range. The 24-hour observed snowfall for the period ending at 12 UTC 18 March is shown in Fig. 24. In this case, the pattern recognition application confirmed indications from the models that a significant snowfall would occur across the southern tier of New York and far northern Pennsylvania. The potential for up to 10 inches of snow indicated by the application was more than what was explicitly forecast by any of the guidance (assuming snow to liquid ratios of 20 to 1 or less), and should have signaled forecasters that an unusual event was about to occur.

4. Summary and Discussion

The increased availability of local models with small horizontal grid spacing has made their utilization increasingly popular during the past several years. At the same time, computational limits and operational needs have resulted in a 5 to 10 km horizontal grid spacing in many of these models. At these resolutions, narrow, multi-bands of lake-effect snow are not explicitly resolved. Therefore, there is still opportunity to apply forecaster experience and pattern recognition to improve over model guidance in the lake-effect snow forecasting process.

The main benefit of the pattern recognition application shown in this paper is to assist in expanding the experience database of all forecasters, by enhancing their ability to relate current

events to historical events through pattern recognition. When experienced forecasters can confirm that output from a model with small horizontal grid spacing matches their experiential expectations given a particular flow regime, forecaster confidence increases, and it becomes easier for the forecaster to correctly anticipate significant or even extreme events. Conversely, if output from a model with small horizontal grid spacing does not match the forecasters expectations based on their experience, this could be taken as a signal to be skeptical of the numerical guidance. Therefore, this application should be particularly useful for less experienced forecasters.

One important aspect of any lake-effect snow event, that is not particularly well-addressed by the pattern recognition application shown in this paper, is event duration. The application is tuned to return "snap-shots" of expected 0.5º radar reflectivity images, given a particular set of expected environmental conditions. The forecaster does have the ability to enter whether or not the expected event will be "persistent," with the definition of a "persistent" event being any event with a mean wind direction varying by less than 10º through a period that is at least 12 hours long. However, this still leaves a wide range of possible event durations that are not accounted for. For example, recall from section 3a that the application once matched a "persistent" current event that remained nearly steady-state for around 12 hours with a historical event that remained nearly steady-state for 48 hours. In that case, the historical event produced much more snow than the current event, making it a poor analogue regarding storm total snowfall. Therefore, forecasters still need to carefully consider the effects of event persistence on total snowfall, since the degree of snow band persistence across a particular location will correlate directly with the amount of snow that accumulates at that location.

One of the more useful features of the pattern recognition application shown in this paper is the ability to display several different historical events corresponding to a current event. The returned historical events usually appear reasonably similar to each other. However there are times when a variety of different looking events are returned. Generally speaking, there are two possible reasons why the returned events may occasionally not appear to be very similar to each other. The first reason would be that the current flow pattern is such that very minor differences in the associated soundings could result in large differences in lake effect snow morphology. In these cases, dissimilar returned events would indicate that the outcome of the current event is highly uncertain, even if the low-resolution model has a reasonably good handle on the large-scale flow pattern. The other possibility is that the current event is unusual, and as a result the database does not contain enough truly similar cases for each returned case to be a good match to the current case. This possibility will become increasingly less likely as additional cases continue to be added to the database.

Finally, the concept of developing a pattern recognition enhancement application based on comparison of parameters associated with current conditions to parameters from analogue events, may have applications in areas other than lake-effect snow forecasting. The key to identifying forecast challenges that would be well suited to this type of approach would be to identify scenarios where models forecast the background environment reasonably well, but do not necessarily make good, explicit forecasts of the phenomena in question. For example, the NWSFO at BGM has been experimenting with developing a similar application to help

anticipate warm-season convective mode. Aviation forecasting could be another area where this type of approach may be appropriate.

The key to developing similar applications for different forecast problems is to identify key attributes of the sounding that modulate the evolution of the phenomena in question. In the case of lake effect snow, the large body of previous research plus a great degree of local operational experience made identifying several key parameters relatively easy. Even so, ongoing local research plus experience with the application will result in the inclusion of additional parameters in the future. As such, this application provides an excellent opportunity to input results from research into operations. In contrast to lake effect snow, other phenomena may be less well understood, and a major research effort may be required prior to the development of a similar application. Once the key parameters are identified, the next steps are to create the database of parameters, derive similarity algorithms, and create the database search application.

Acknowledgements

The authors would like to thank the NWS at Buffalo, NY for the use of their 6 km WRF model in the case studies. In addition, we would like to thank BGM forecasters Michael Jurewicz and Robert Mundschenk for helping to develop and quality control the historical database. Finally, we would like to thank BGM forecaster Justin Arnott, ER SSD meteorologists Jeff Waldstreicher and Dave Novak, and two anonymous reviewers, for reviewing this manuscript.

Authors

Mike Evans has been the science operations officer at the National Weather Service Forecast Office in Binghamton, NY since 2002. Before coming to BGM, Mike worked in the National Weather Service as an intern in Charleston, WV, a journeyman forecaster in White Lake, Michigan, and a lead forecaster in State College, Pa. Mike received a B.S. in Meteorology from Penn State in 1985, and an M.S. in Atmospheric Science from SUNY Albany in 1992.

Ron Murphy has been the information technology officer at the National Weather Service Forecast Office in Binghamton, NY, since 2003. Before holding his current position, Ron was a National Weather Service intern in Lake Charles La, a journeyman and lead forecaster at Birmingham, AL, and a lead forecaster at Binghamton. Ron received a B.S. in Meteorology from SUNY Oswego in 1987.

References

Ballentine R. J., A. J. Stamm, E. E. Chermack, G. P. Byrd, and D. Schleede 1998: Mesoscale Model Simulation of the 4–5 January 1995 Lake-Effect Snowstorm *Wea. Forecasting*, **13**, 893–920

Benjamin S.G., D. Dévényi, S. S. Weygandt, K. J. Brundage, J. M. Brown, G. A. Grell, D. Kim, B. E. Schwartz, T. G. Smirnova, T. L. Smith, and G. S. Manikin: 2004: An Hourly Assimilation–Forecast Cycle: The RUC. *Mon. Wea. Rev.*, **132**, 495–518.

Byrd, G.P., R.A., Anstett, J.E. Heim, and D. M. Usinski, 1991: Mobile sounding observations of lake-effect snowbands in western and central New York, *Mon. Wea. Rev.*, **119**, 2323-2332.

Dockus, D.A., 1985: Lake effect snow forecasting in the computer age. *Natl. Wea. Dig.*, **10**, 5-19.

Ferrier, B.S., Y. Jin, T. Black, E. Rogers, and G. DiMego, 2002: Implementation of a new grid-scale cloud and precipitation scheme in the NCEP Eta model, Preprints, 15th Conference on Numerical Weather Predication, San Antonio TX, Amer. Meteor., Soc., 280-283.

Gallus, W.A., 1999: Eta Simulations of three extreme precipitation events: sensitivity to resolution and convective parameterization. *Wea. Forecasting*, **14**, 405-426.

Janjic, Z. I., 1996: The Mellor-Yamada level 2.5 scheme in the NCEP Eta Model. Preprints, 11th Conference on Numerical Weather Prediction, Norfolk, VA., Amer. Meteor. Soc. 333-334.

Kolker, B., 1978: Current forecast procedures for lake effect snow in western New York especially related to the 1976-1977 and 1977-1978 winters. *Proc. of the 35th Ann. Eastern Snow Conf.*, Hanover, NH, 17-35. [Available from United States Army, CRREL, 72 Lyme Rd., Hanover, NH, 03755]

Kristovich, D.A.R., and M.L. Spinar, 2004: Observations of the diurnal evolution of lake-effect precipitation occurrence, Preprints, 14th Conference on Applied Climatology, Seattle WA, Amer. Meteor. Soc., P5.2, 3pp.

Lackmann, G. M., 2001: Analysis of a surprise western New York snowstorm. *Wea. and Forecasting*, **16**, 99-116.

Laird, N.F., J. E. Walsh, and D. A. R. Kristovich, 2003: Model simulations examining the relationship of lake-effect morphology to lake shape, wind direction, and wind speed. *Mon. Wea. Rev.* **131**, 2102–2111

Mahoney, E. A., and T. A. Niziol, 1997: BUFKIT: A software application toolkit for predicting lake-effect snow. *Preprints 13th Intl. Conf. on Interactive Information and Processing Systems for Meteorology, Oceanography, and Hydrology*, Long Beach, CA, Amer. Meteor. Soc., 388-391.

Niziol, T.A., W.R. Snyder, J.S. Waldstreicher, 1995: Winter weather forecasting throughout the eastern United States, Part IV: lake effect snow, *Wea. Forecasting.* **10**, 61-77.,

_____ 2003: An analysis of satellite-derived Great Lakes surface temperatures in regards to model simulations of lake effect snow. Preprints, 10th Conference on Mesoscale Processes, Portland OR, Amer. Meteor., Soc., P1.9, 6pp.

Reinking, R.F., R.A., Kropfli, B.E. Martner, B. Orr, J. B. Snider, T. Uttal, R.J. Zamora, R. Caiazza, R. Maraio, R.S. Penc, A. Koscielny, G.P. Byrd, T.A. Niziol, R. Ballentine, A. Stamm, R. Sykes, C. Bedford, P. Joe and A. Eschner, 1991: Lake Ontario winter storms (LOWS) project final report. NOAA Tech Memo. E.R.L. WPL-216, NOAA/WPL, Boulder, CO 147 pp.

Rogers, E. T., Black, B. Ferrier, Y. Lin, D. Parrish, and G. DiMego, 2001: Changes to the NCEP Meso-Eta analysis and forecast system: increase in resolution, new cloud microphysics, modified precipitation assimilation, modified 3DVAR analysis. NOAA/NWS Technical Procedures Bulletin 488, 21 pp.
[Available online at http://www.emc.ncep.noaa.gov/mmb/mmbpll/eta12tpb/]

Rothrock, H.J., 1960: An aid in forecasting significant lake snows, ESSA Tech Memo, WBTM CR-30, NOAA/NWS, Kansas City, MO, 18 pp.

Sobash, R.H., H. Carr and N.F. Laird, 2005: An investigation of New York State Finger Lakes snow band events, Preprint, 11th Conference on Mesoscale Processes, Albuquerque, NM, Amer. Meteor. Soc., P3M.3, 5pp.

Sousounis, P.J. and G.E. Mann, 2000: Lake-aggregate mesoscale disturbances. Part V: Impacts on lake effect precipitation. *Mon. Wea. Rev*. **81**, 223-236.

Watson, J.S., M.L.Jurewicz, R. Ballentine, S. Colucci, and J.S.Waldstreicher, 1998: High resolution numerical simulations of finger lakes snow bands.. Preprints, 16th Conference on Weather Analysis and Forecasting, Phoenix, AZ., Amer. Meteor. Soc., 308-310.

Weisman, M. L., W. C. Skamarock, and J. B. Klemp, 1997: The resolution dependence of explicitly modeled convective systems. *Mon. Wea. Rev*., **125**, 527-548.

Zavisa, I.J, 2004: The NCEP WRF core, Preprint, 20th Conference on Weather Analysis and Forecasting/16th Conference on Numerical Weather Prediction, Seattle, WA, Amer. Meteo. Soc, P12.7, 21 pp.

APPENDIX

The algorithm to identify historical events that are "most similar" to the current event is a point system. Each event in the database is compared to the current event, and assigned points based on the similarity of its sounding parameters to the corresponding parameters of the current event. The events with the most points are returned as being "most similar". Before points are assigned, a large number of historical events are eliminated from consideration using the following rules:

If the difference in mean wind direction between the historical case and current case is greater than 10 degrees, remove the historical case from consideration.

If the level of the base of the inversion of the current case is above 750 hPa, and the level of the base of the inversion of the historical case is below 880 hPa remove the historical case from consideration.

If the level of the base of the inversion of the current case is below 880 hPa and the level of the base of the inversion of the historical case is above 750 hPa, remove the historical case from consideration.

If the difference in the depth of the moist layer (defined by all layers where the dew point depression is 3 º C or less) between the historical case and the current case is greater than 200 hPa, remove the historical case from consideration.

Once this subset of historical cases has been removed from consideration, points are assigned to the remaining events by the criteria in table A1:

Table A1. A summary of the point system used to determine the most similar historical events in the pattern recognition application described in this paper.

Parameter	Assign 5 points to the historical event	Assign 4 points to the historical event	Assign 3 points to the historical event	Assign 2 points to the historical event	Assign 1 point to the historical event
Mean wind direction in the mixed layer	< 5 degrees			5-10 º	
Mean wind speed			< 10 kts	10-15 kts	16-20 kts
850 hPa temperature			< 5 º	5-8 º	9-15 º
850 hpa / Lake temperature diff.			< 5 º	5-8 º	9 to 15 º
Inversion base level		< 20 hPa	20-40 hPa	41-80 hPa	81-150 hPa
Moisture depth			< 41 hPa	41-80 hPa	81-150 hPa
Dendritic growth Zone depth			< 41 hPa	41-80 hPa	81-150 hPa
Max lift in the Dendritic growth Zone *			< 6 μbs^{-1}	6-10 μbs^{-1}	11-15 μs^{-1}
Max Tdd below 900 hPa			< 3 º		3-4 º
RMS Shear			≤ 0.5	0.51 – 1.00	1.01 – 1.5
Persistence			Both are persistent Both are not		
Time of day				Match**	

* The point thresholds for this parameter would have to be adjusted when using data from grids with significantly higher or lower resolution than the 12 km NAM or 13 km RUC.

** A match for time of day is defined as follows: If the current time is 00 UTC, a historical time of 18 UTC or 00 UTC is a match. If the current time is 06 UTC, a historical time of 06 UTC or 12 UTC is a match. If the current time is 12 UTC, a historical time of 06 UTC or 12 UTC is a match. If the current time is 18 UTC, a historical time of 18 UTC or 00 UTC is a match.

Algorithm for objectively determining the base of the subsidence inversion

Inversions are typically defined as layers where the temperature increases with height. However, in the case of lake effect snow forecasting, we have observed that forecasters do not use this strict definition of an inversion when determining the height of the subsidence inversion. Instead, we have observed that forecasters subjectively define the subsidence inversion as a layer where subsidence is indicated by drying and a decreased (but not necessarily negative) lapse rate. In addition, we found that forecasters often ignore very shallow, surface-based inversions. For this application, we decided to define the subsidence inversion height objectively, using an algorithm that produces a result that matches what forecasters would set as the subsidence inversion as closely as possible. After considerable trial and error, the following algorithm was developed:

Define ΔT as the temperature at the current level subtracted from the temperature at the next level above the current level in the BUFR data. For example, if temperature increases with height, ΔT is positive.

Start sampling at the level closest to 950 hPa and repeat the following at every level until an inversion is defined, or until you reach the level closest to 850 hPa.

If $\Delta T >= 0$ set this as your inversion level.

If $\Delta T < 0$ but $> - 0.4$ then check the value of the dew point depression.

If the dew point depression >= 5C, then set this as your inversion level.

If $\Delta T <= -0.4$, you have no inversion

If no inversion has been defined by the time you have sampled up to 850 hPa, do the following at each layer until you define an inversion, or until you reach the layer closes to 500 hPa.

If the dew point depression >= 5C then set this as your inversion level.

If delta T > -0.8 set this as your inversion level.

If no subsidence inversion level has been defined before reaching 500 hPa, set the inversion level at 500 hPa.

Figures

Fig. 1. Domain for the WRF model run at the NWS forecast office at Buffalo, NY. Note that the domain was chosen to capture the effects of Lakes Erie, Ontario and Huron.

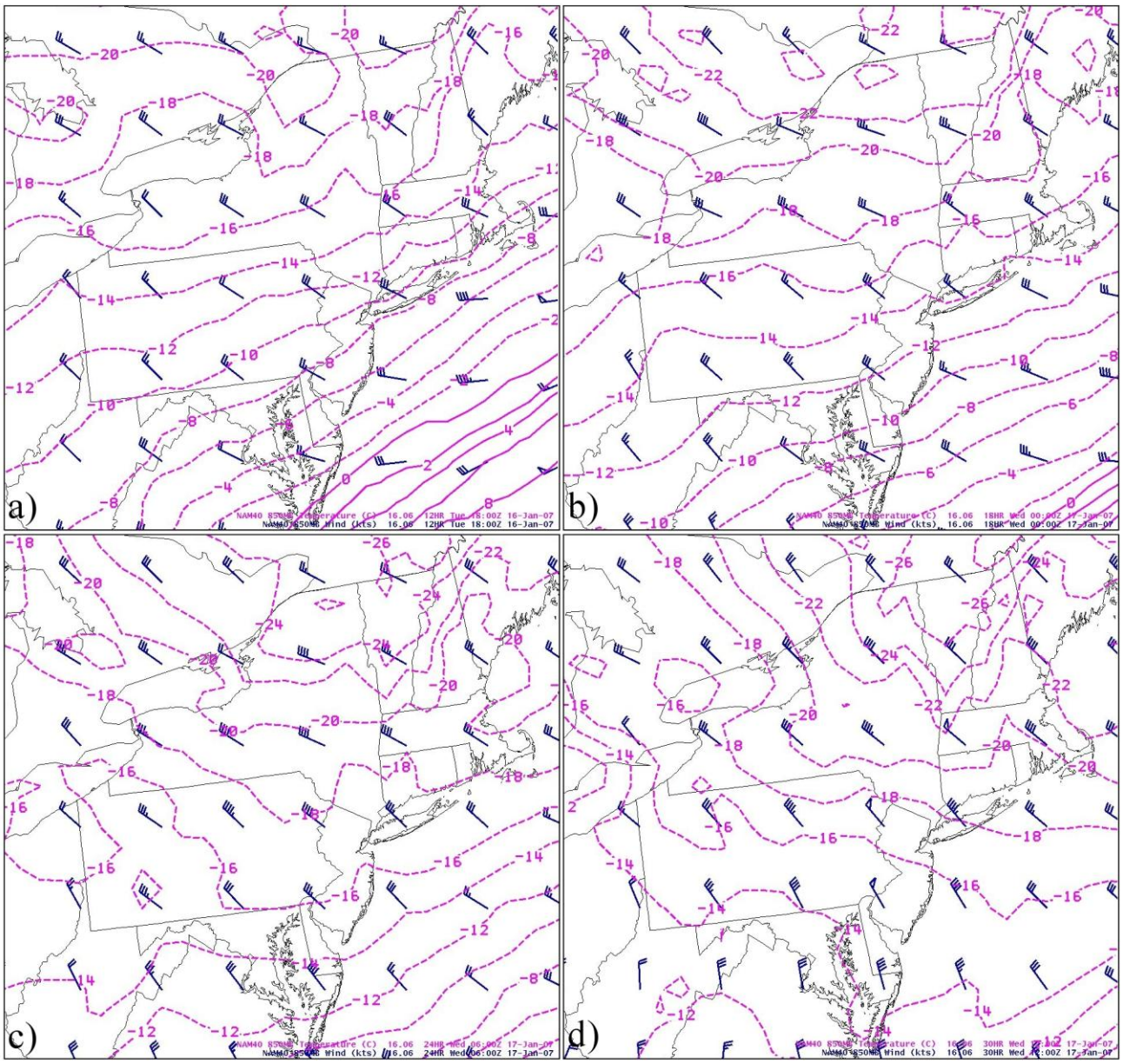

Fig. 2. 12 UTC 16 January 2007 NAM 850 hPa wind (kts) and temperature (ºC) valid at a) 18 UTC 16 Jan. 2007, b) 00 UTC 17 Jan. 2007, c) 06 UTC 17 Jan. 2007 and d) 12 UTC, 17 Jan. 2007.

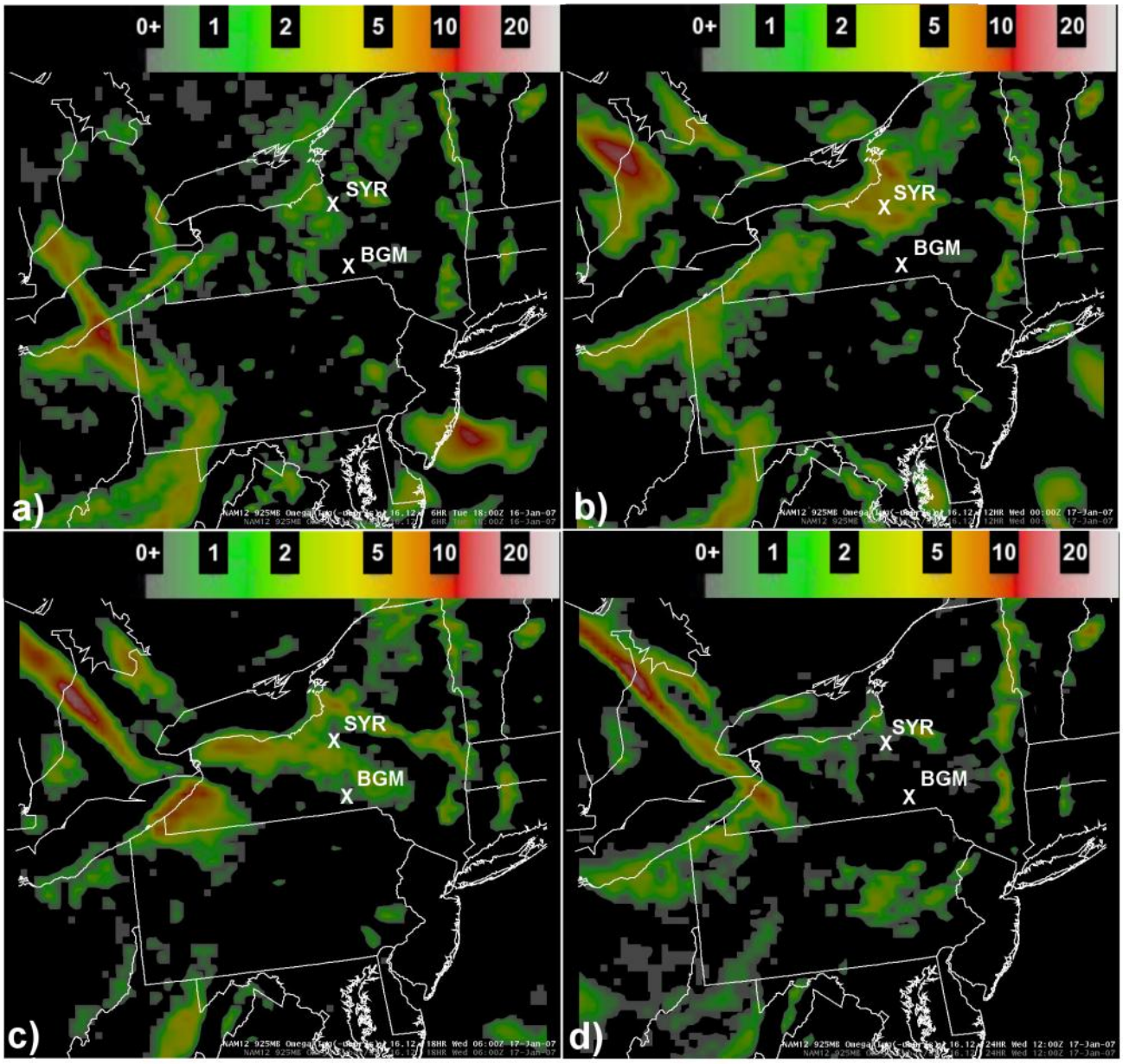

Fig. 3. 12 UTC 16 January 2007 NAM 925 hPa omega ($-\mu bs^{-1}$), with upward vertical motion shaded, valid at a) 18 UTC 16 Jan. 2007, b) 00 UTC 17 Jan. 2007 c) 06 UTC 17 Jan. 2007 and d) 12 UTC 17 Jan. 2007.

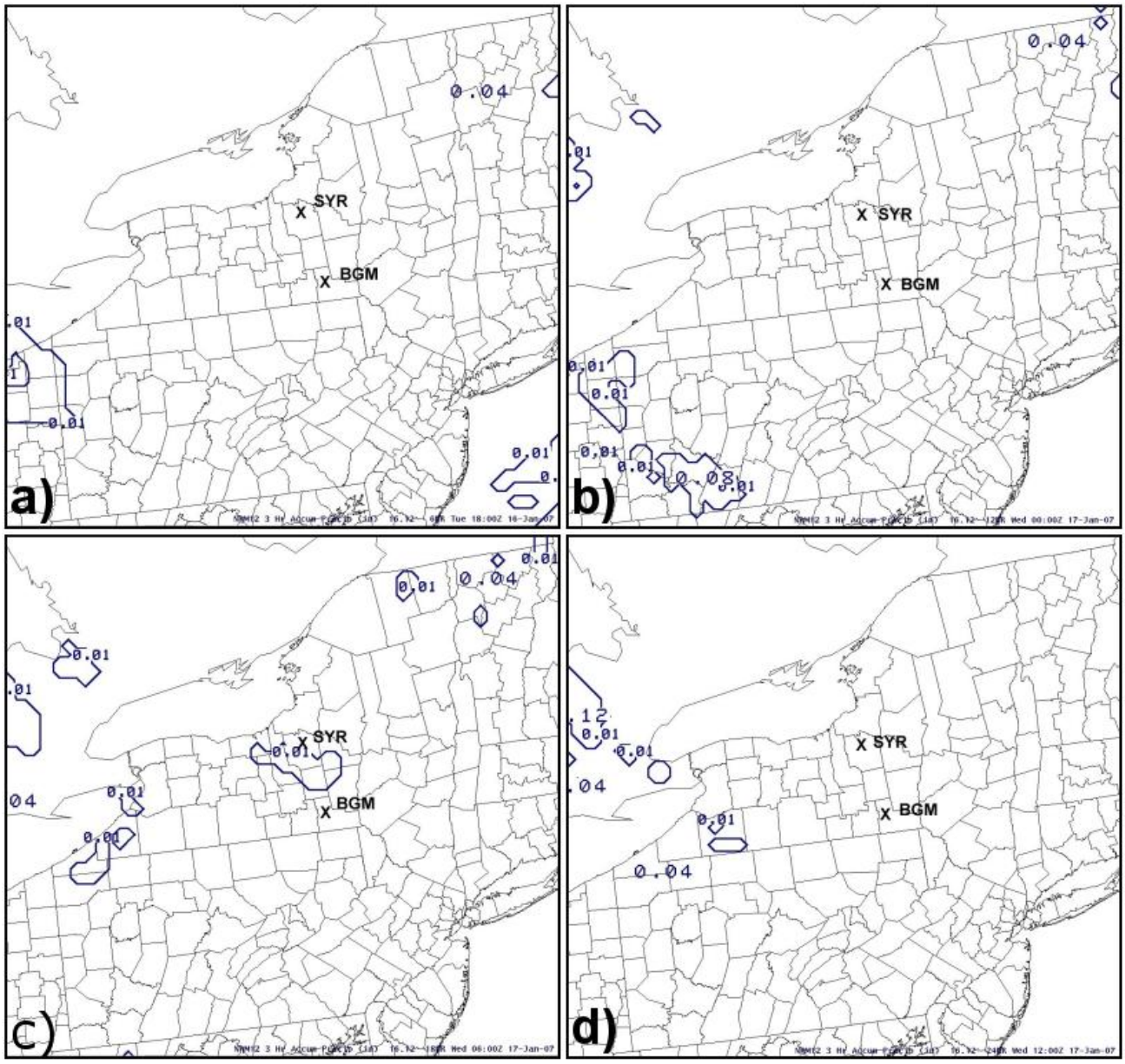

Fig. 4. 12 UTC 16 January 2007 NAM forecast 3-hour quantitative precipitation (inches) valid at a) 18 UTC Jan. 16 2007, b) 00 UTC Jan. 17 2007, c) 06 UTC Jan. 17 2007 and d) 12 UTC Jan. 17 2007.

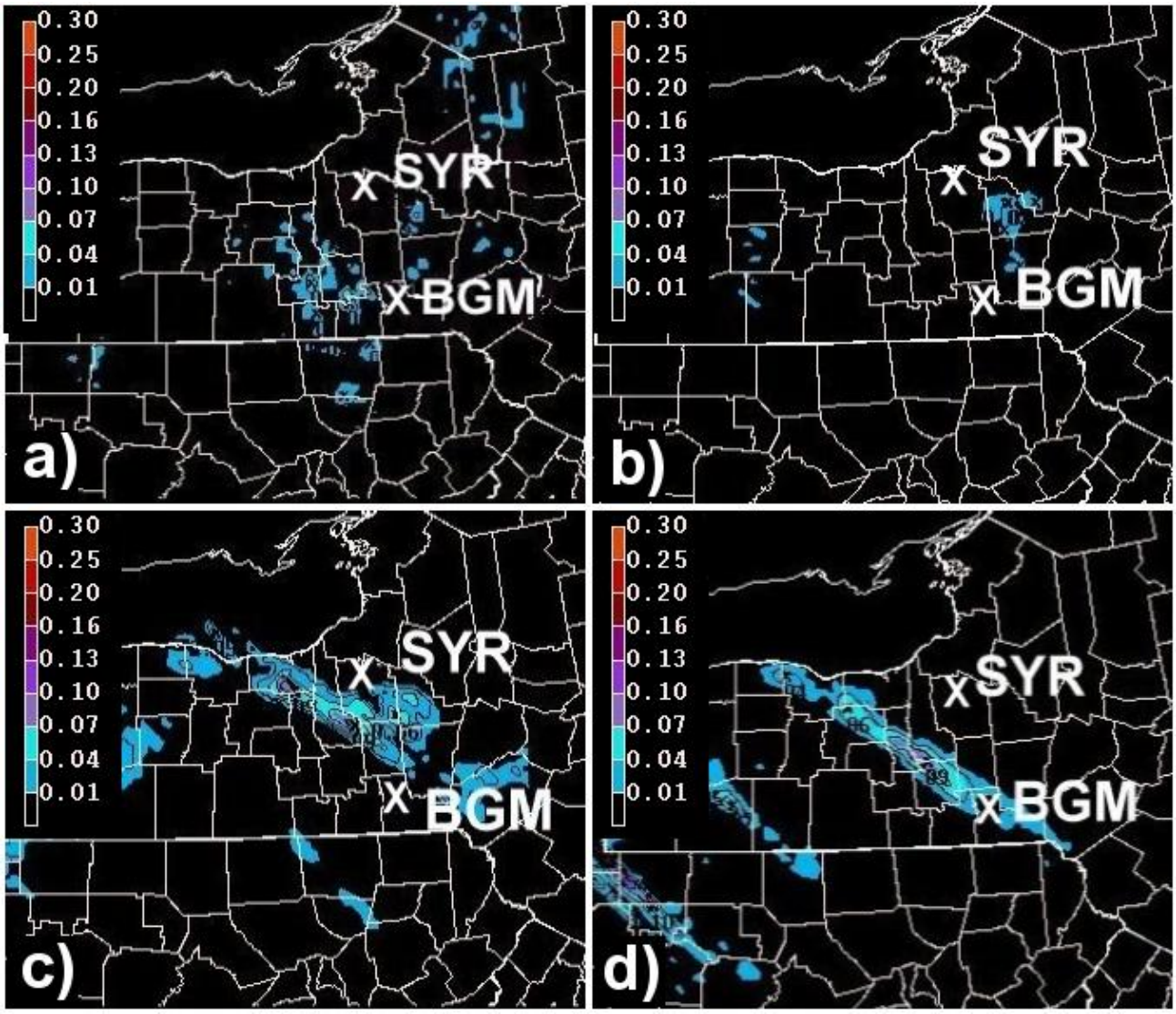

Fig. 5. 12 UTC 16 January 2007 6 km Workstation (or local) WRF 6-hour quantitative precipitation forecasts (inches) valid at a) 18 UTC 16 Jan. 2007, b) 00 UTC 17 Jan. 2007, c) 06 UTC 17 Jan. 2007 and d) 12 UTC 17 Jan. 2007.

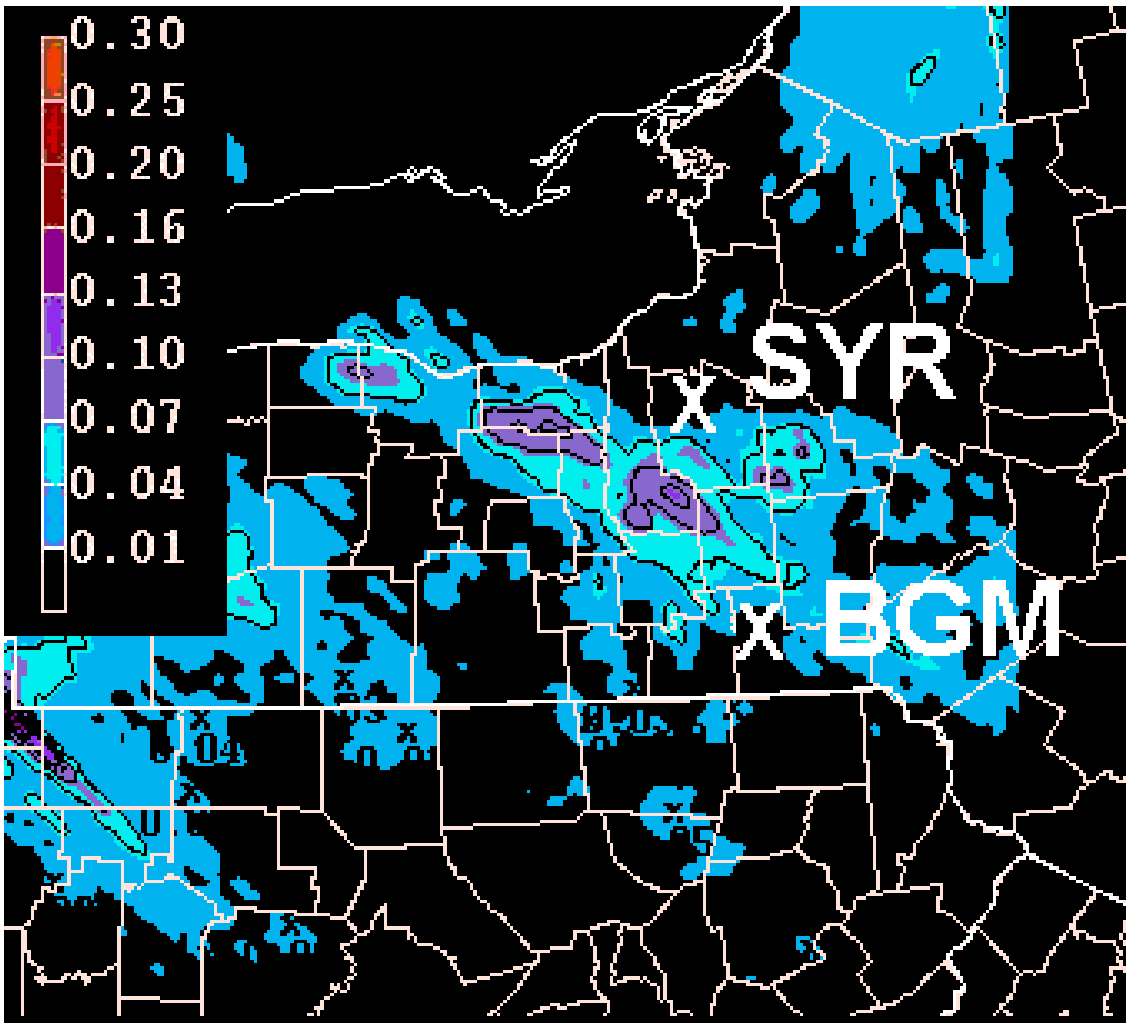

Figure 6. 12 UTC 16 January 2007 6-km WRF 24-hour quantitative precipitation (inches) forecast valid at 12 UTC 17 Jan. 2007.

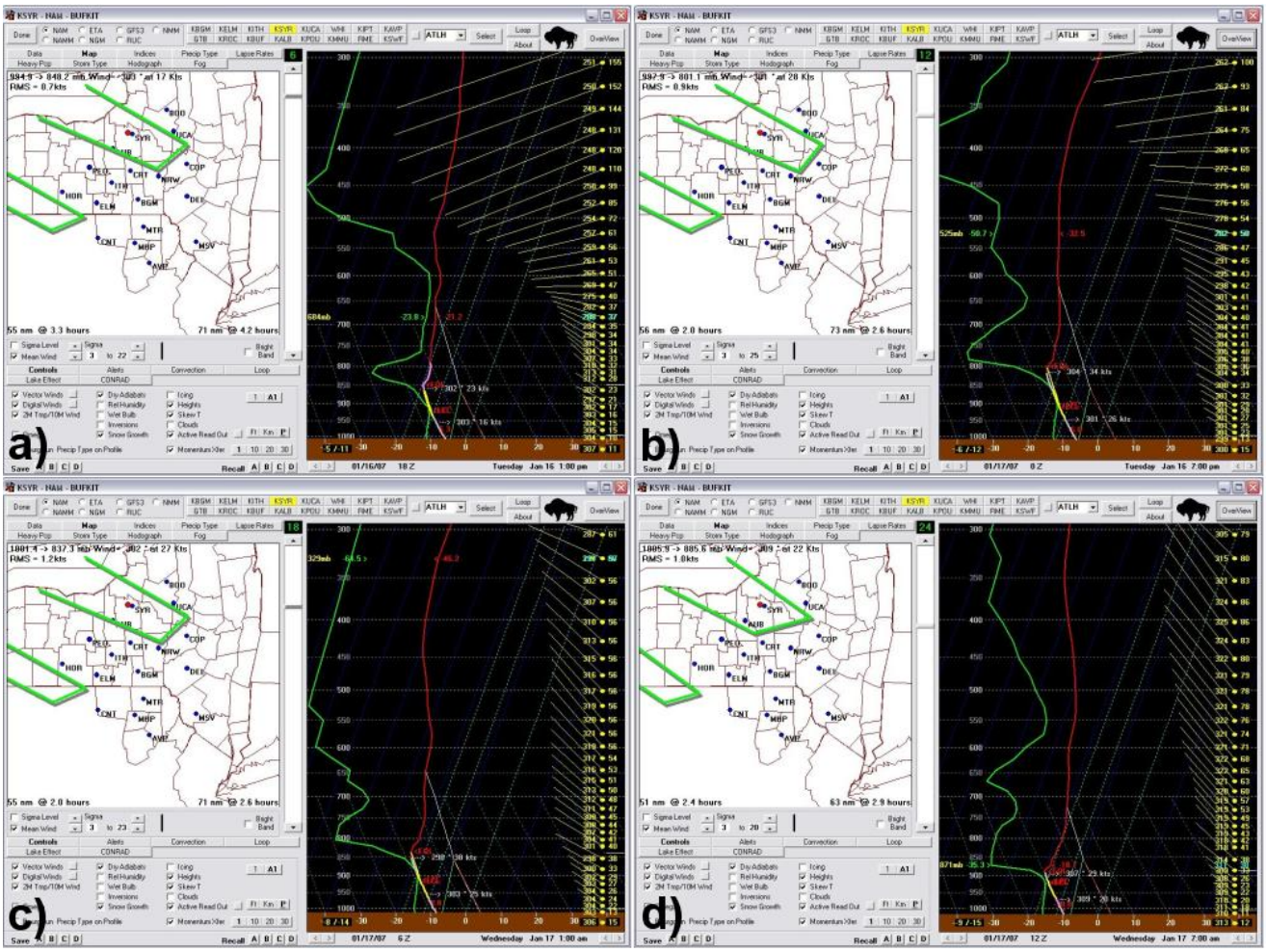

Fig. 7. 12 UTC 16 January 2007 NAM model forecast soundings valid at SYR as displayed by BUFKIT software and valid at a) 18 UTC 16 Jan. 2007, b) 00 UTC 17 Jan. 2007, c) 06 UTC 17 Jan. 2007 and d) 12 UTC 17 Jan. 2007.

LES Checklist Results	Similar Events for Site: SYR 1800 UTC					
Parameter	Your Values	Values 02/18/2005 at 1800 UTC	Values for 12/14/2004 at 1800 UTC	Values for 03/03/2005 at 1800 UTC	Values for 12/17/2004 at 1800 UTC	Values for 03/20/2006 at 0000 UTC
Mean Wind Direction:	303	307	301	305	305	305
Mean Wind Speed (knots):	17	22	15	18	20	19
850 mb Temperature (°C):	-18	-22	-14	-16	-15	-15
Lake - 850 mb Temperature Difference (°C):	24	24	20	18	19	18
Inversion Height (mb):	850	875	890	890	890	850
Moisture Depth (mb):	120	150	130	110	110	220
Dendritic Depth (mb):	60	80	40	60	20	130
Max Omega in the Dendritic Zone:	0	-5	-4	-4	-4	-4
Max Tdd below 900 mb:	5	3	4	3	3	3
RMS Wind:	0.7	0.6	0.8	0.9	0.6	1.1
Persistent:	no	no	no	no	no	no
a)		Show 02/18/2005 at 1800 UTC	Show 12/14/2004 at 1800 UTC	Show 03/03/2005 at 1800 UTC	Show 12/17/2004 at 1800 UTC	Show 03/20/2006 at 0000 UTC

LES Checklist Results	Similar Events for Site: SYR 0000 UTC					
Parameter	Your Values	Values 01/11/2007 at 0000 UTC	Values for 02/07/2006 at 1800 UTC	Values for 12/08/2006 at 0000 UTC	Values for 12/20/2006 at 0000 UTC	Values for 02/27/2006 at 0000 UTC
Mean Wind Direction:	301	304	298	305	304	311
Mean Wind Speed (knots):	28	28	17	23	23	27
850 mb Temperature (°C):	-19	-16	-13	-17	-9	-20
Lake - 850 mb Temperature Difference (°C):	25	22	15	24	16	21
Inversion Height (mb):	800	770	870	800	730	750
Moisture Depth (mb):	130	210	160	330	240	170
Dendritic Depth (mb):	80	80	70	70	70	80
Max Omega in the Dendritic Zone:	-4	-3	-3	-1	-2	-12
Max Tdd below 900 mb:	6	4	3	3	6	4
RMS Wind:	0.9	1.9	1.1	1.1	0.8	1.3
Persistent:	yes	no	yes	no	no	no
b)		Show 01/11/2007 at 0000 UTC	Show 02/07/2006 at 1800 UTC	Show 12/08/2006 at 0000 UTC	Show 12/20/2006 at 0000 UTC	Show 02/27/2006 at 0000 UTC

LES Checklist Results	Similar Events for Site: SYR 0600 UTC					
Parameter	Your Values	Values 11/18/2005 at 0600 UTC	Values for 03/04/2005 at 0600 UTC	Values for 03/16/2006 at 0600 UTC	Values for 11/14/2003 at 1200 UTC	Values for 12/27/2006 at 1200 UTC
Mean Wind Direction:	302	300	298	299	302	302
Mean Wind Speed (knots):	28	24	22	29	32	20
850 mb Temperature (°C):	-21	-12	-16	-13	-12	-10
Lake - 850 mb Temperature Difference (°C):	27	20	18	16	19	17
Inversion Height (mb):	820	770	830	830	860	770
Moisture Depth (mb):	120	140	170	260	80	140
Dendritic Depth (mb):	70	40	70	110	10	40
Max Omega in the Dendritic Zone:	-1	-6	-11	-6	-10	2
Max Tdd below 900 mb:	6	5	2	2	4	4
RMS Wind:	1.3	1.3	1.7	1.4	1.2	1.2
Persistent:	yes	yes	yes	yes	yes	no
c)		Show 11/18/2005 at 0600 UTC	Show 03/04/2005 at 0600 UTC	Show 03/16/2006 at 0600 UTC	Show 11/14/2003 at 1200 UTC	Show 12/27/2006 at 1200 UTC

LES Checklist Results	Similar Events for Site: SYR 1200 UTC					
Parameter	Your Values	Values 02/08/2004 at 1200 UTC	Values for 03/03/2005 at 1200 UTC	Values for 02/28/2006 at 1200 UTC	Values for 11/26/2004 at 0600 UTC	Values for 03/04/2006 at 1200 UTC
Mean Wind Direction:	309	311	318	305	309	312
Mean Wind Speed (knots):	22	13	18	16	22	24
850 mb Temperature (°C):	-19	-20	-15	-20	-12	-11
Lake - 850 mb Temperature Difference (°C):	25	22	17	21	19	13
Inversion Height (mb):	890	950	910	770	760	900
Moisture Depth (mb):	70	20	90	0	80	190
Dendritic Depth (mb):	50	30	90	0	80	70
Max Omega in the Dendritic Zone:	0	-2	-4	0	-4	-7
Max Tdd below 900 mb:	6	8	5	6	5	2
RMS Wind:	1.0	1.1	1.1	1.7	1.7	1.3
Persistent:	no	no	no	no	no	no
d)		Show 02/08/2004 at 1200 UTC	Show 03/03/2005 at 1200 UTC	Show 02/28/2006 at 1200 UTC	Show 11/26/2004 at 0600 UTC	Show 03/04/2006 at 1200 UTC

Fig. 8. Tabular output from the WFO BGM pattern recognition application for forecasts valid at a) 18 UTC 16 Jan. 2007, b) 00 UTC 17 Jan. 2007, c) 06 UTC 17 Jan.2007, and d) 12 UTC 17 Jan. 2007.

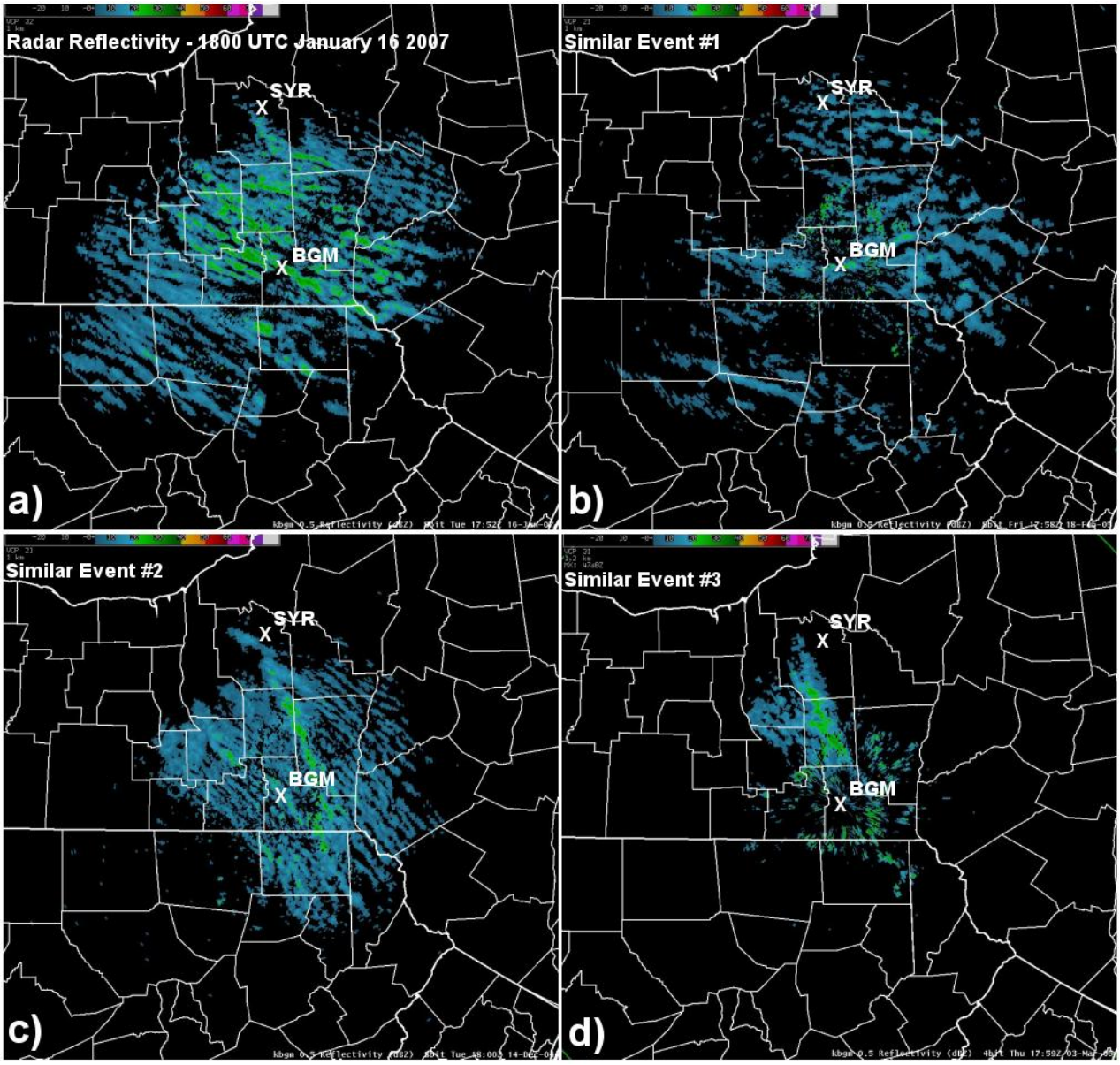

Fig. 9. (a) Observed radar 0.5º reflectivity from the case study at 18 UTC 16 January. 2007; (b-d) Imagery from 3 corresponding similar events selected by the pattern recognition application.

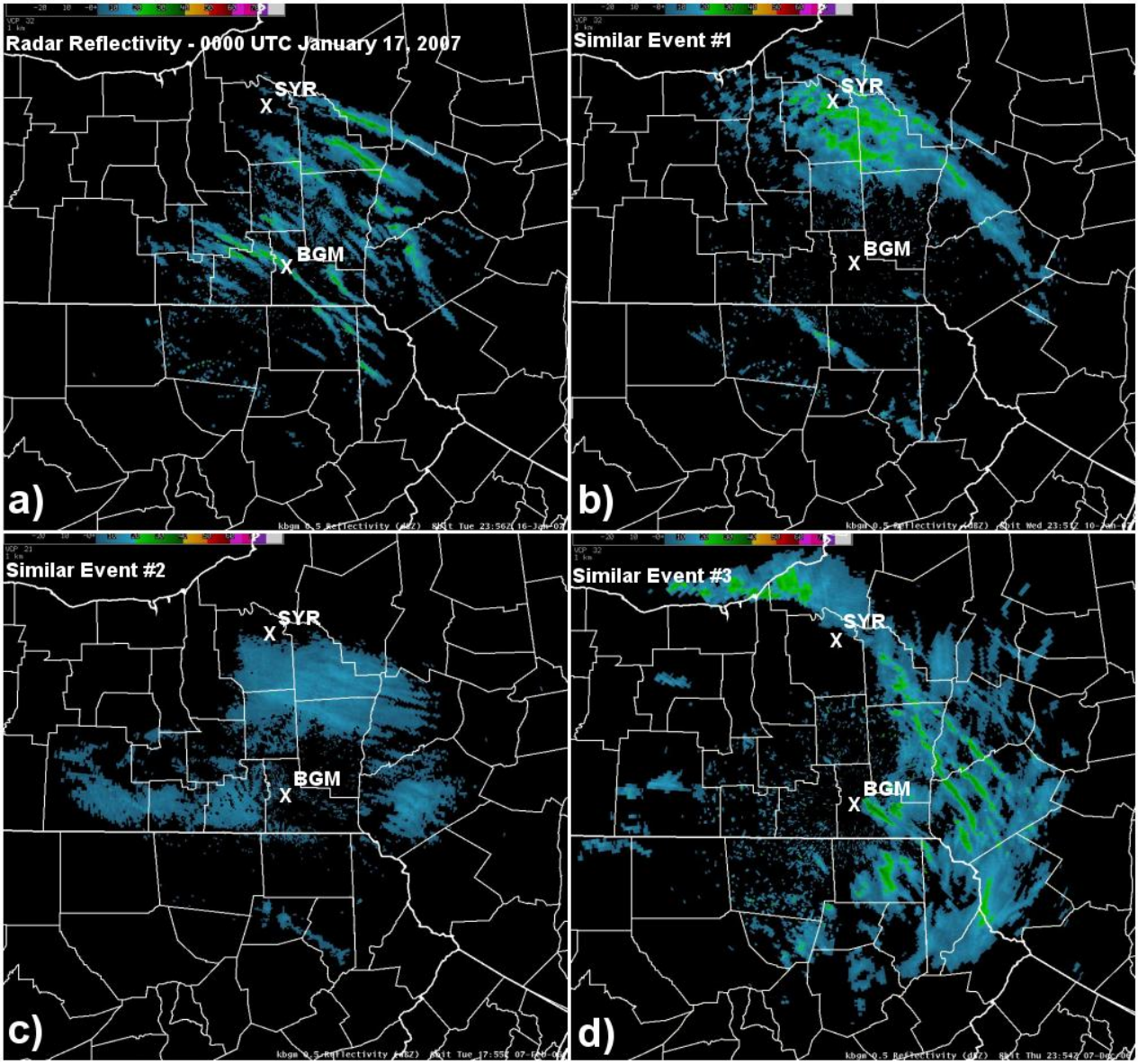

Fig. 10. (a) Observed 0.5º radar reflectivity from the case study at 00 UTC 17 January 2007; (b-d) Imagery from 3 corresponding similar events selected by the pattern recognition application.

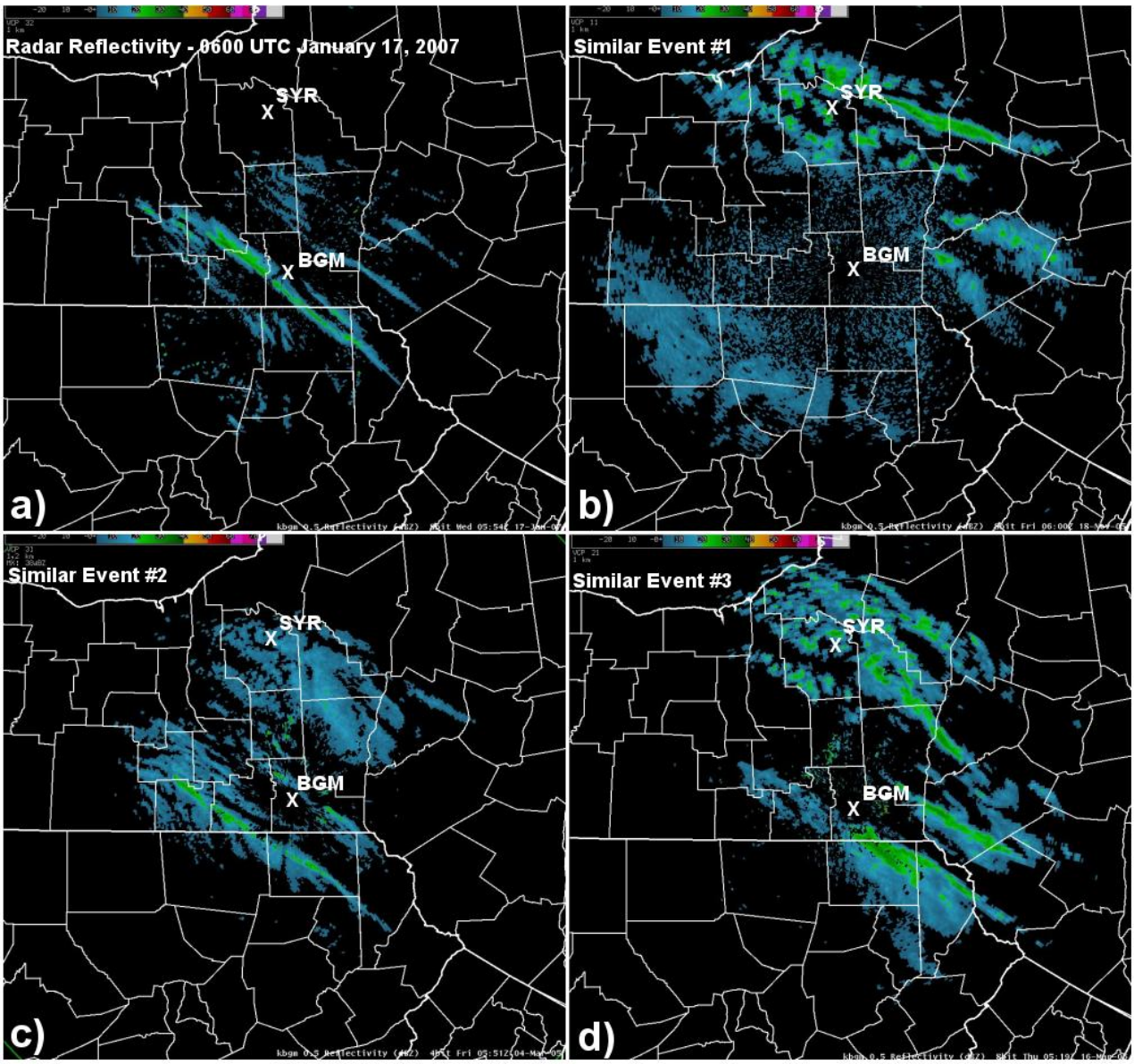

Fig. 11. (a) Observed 0.5º radar reflectivity from the case study at 06 UTC 17 January 2007; (b-d) Imagery from 3 corresponding similar events selected by the pattern recognition application.

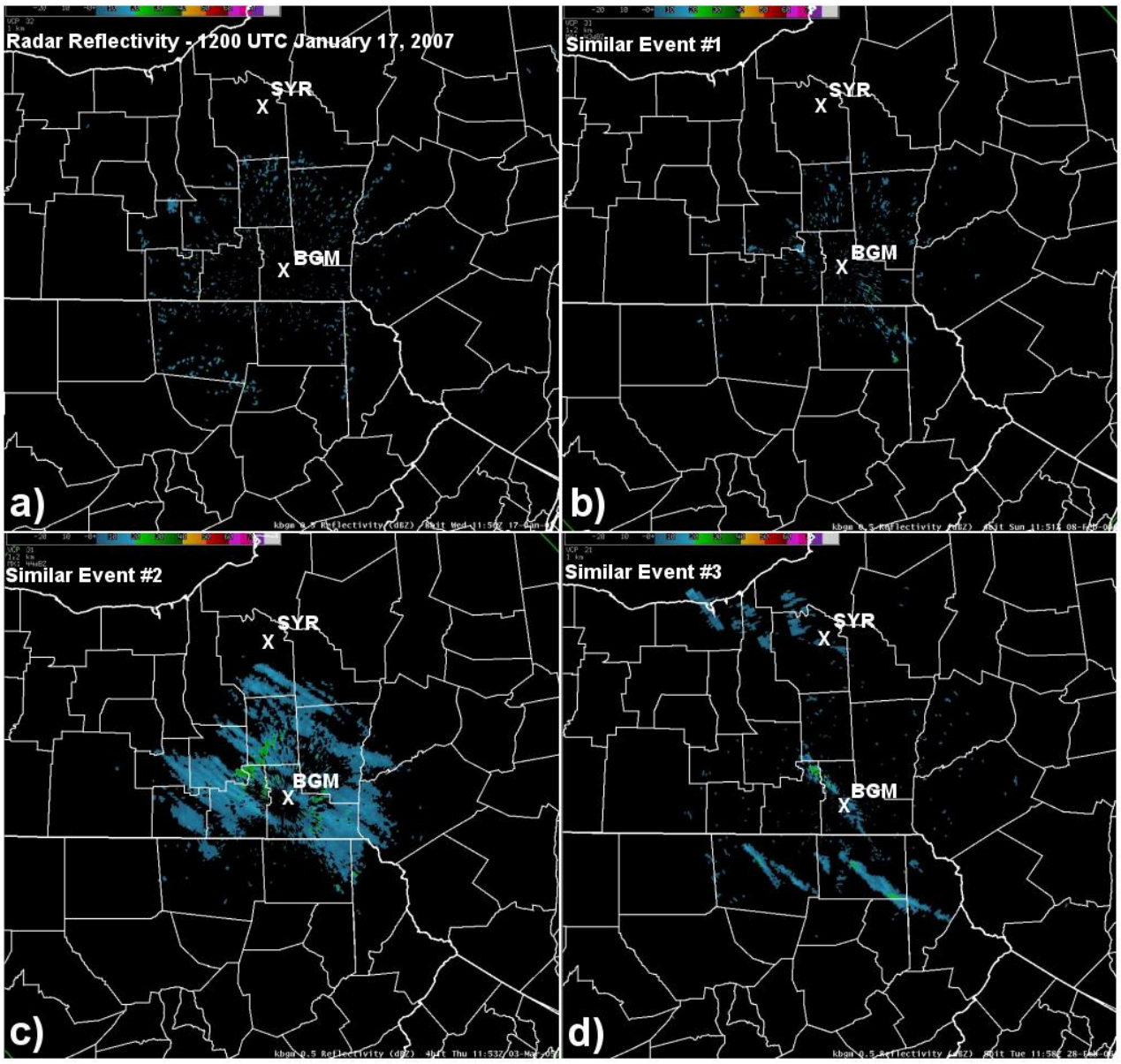

Fig. 12. (a) Observed 0.5º radar reflectivity from the case study at 12 UTC 17 January 2007; (b-d) Imagery from 3 corresponding similar events selected by the pattern recognition application.

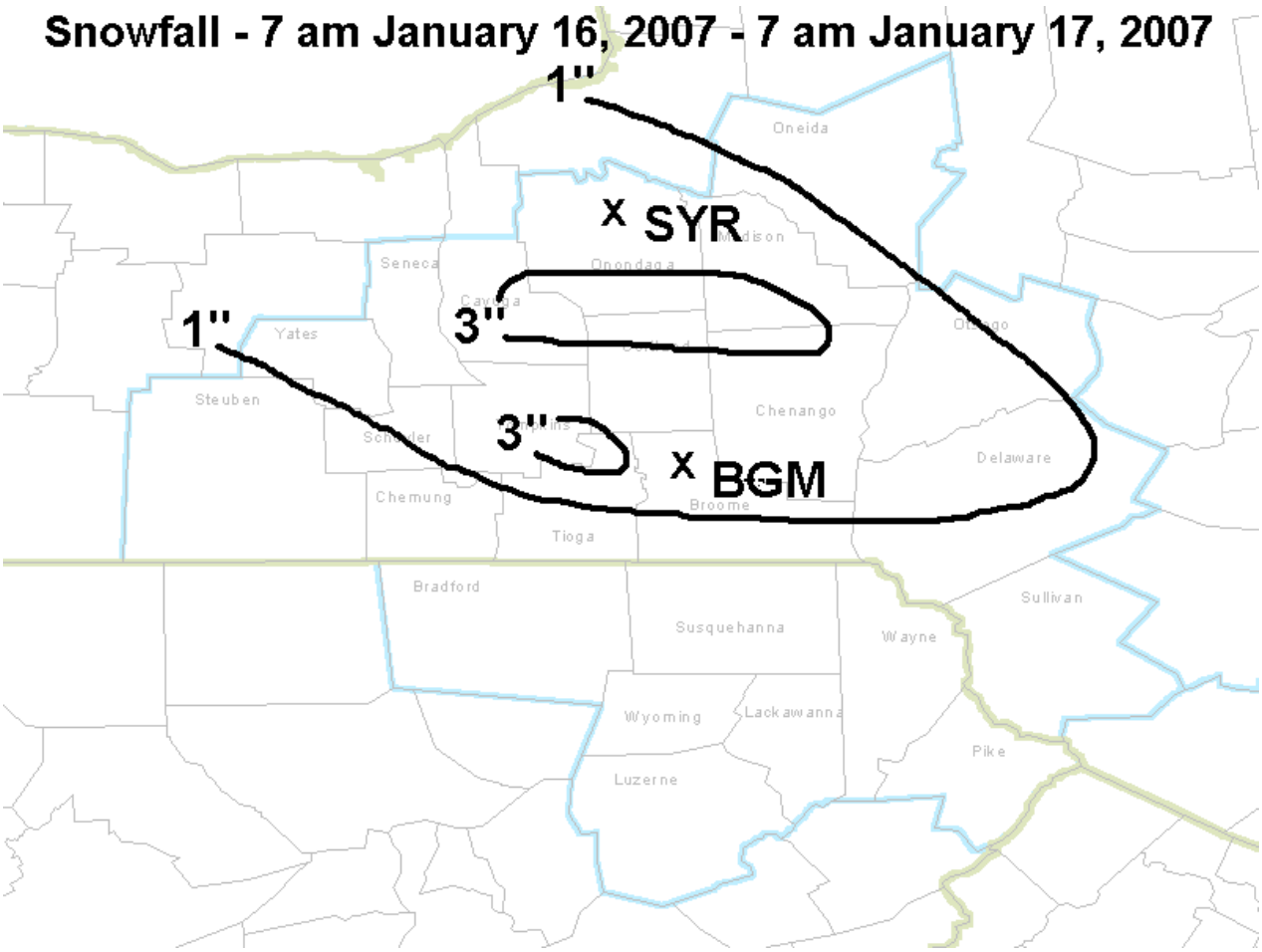

Fig. 13. Observed snowfall (inches) from 12 UTC 16 January 2007 through 12 UTC 17 January 2007.

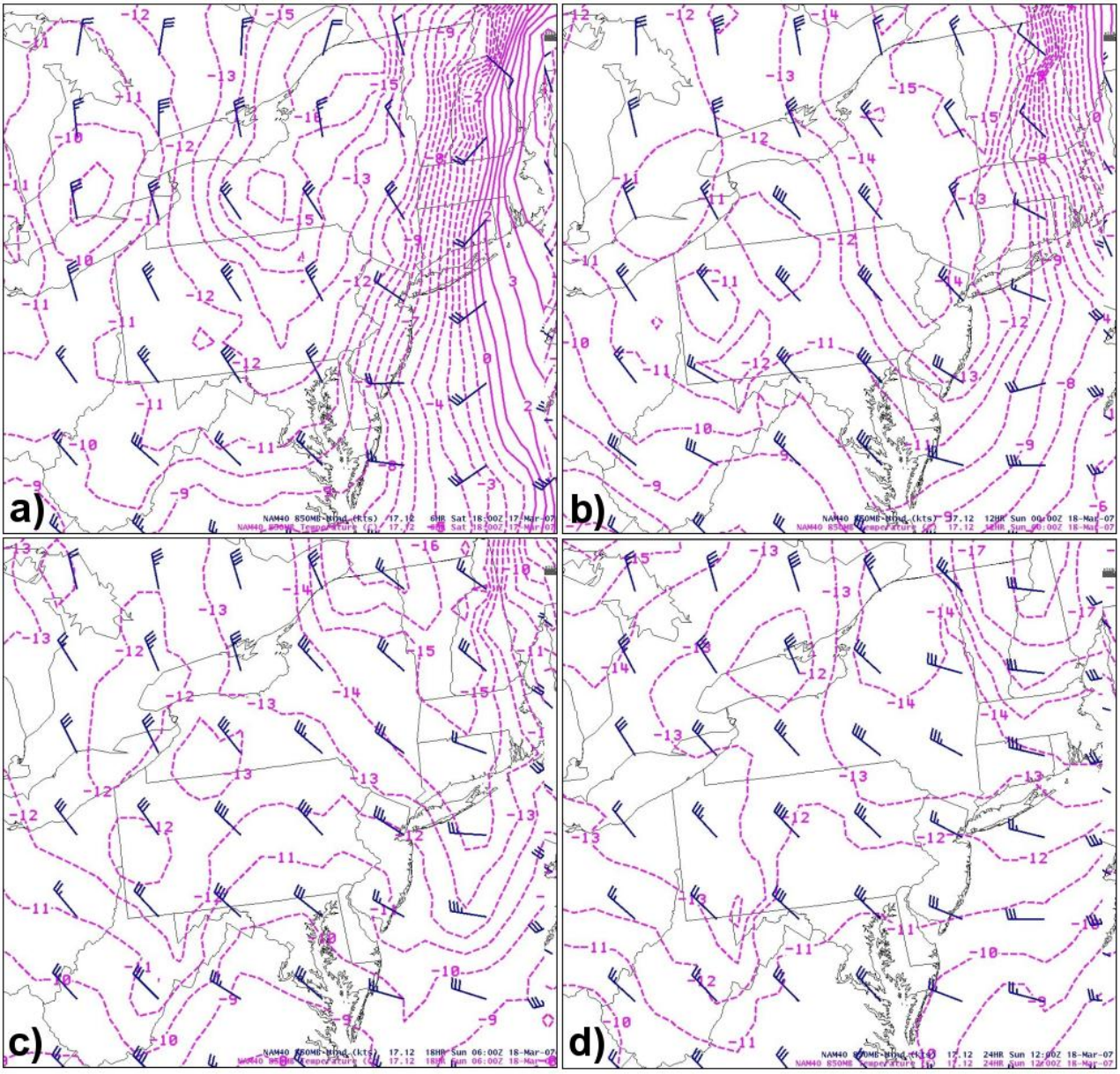

Fig. 14. 12 UTC 17 March 2007 NAM 850 hPa wind (kts) and temperature (ºC) valid at a) 18 UTC 17 Mar. 2007, b) 00 UTC 18 Mar. 2007 c) 06 UTC 18 Mar. 2007, and d) 12 UTC 18 Mar. 2007.

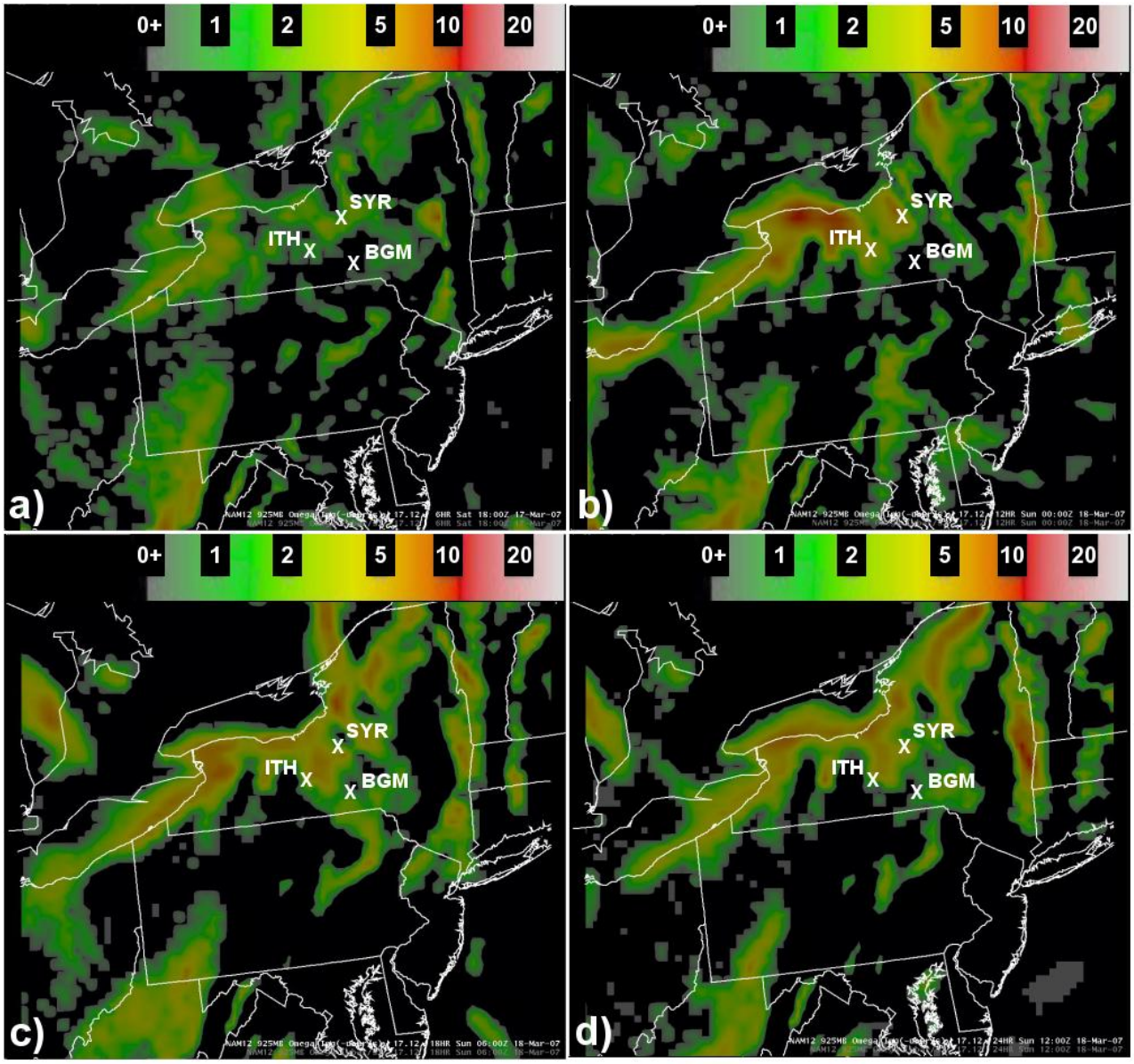

Fig. 15. 12 UTC 17 March 2007 850 hPa omega ($-\mu bs^{-1}$), with upward vertical motion shaded, valid at a) 18 UTC 17 Mar. 2007 b) 00 UTC 18 Mar. 2007, c) 06 UTC 18 Mar. 2007 and d) 12 UTC 18 Mar. 2007.

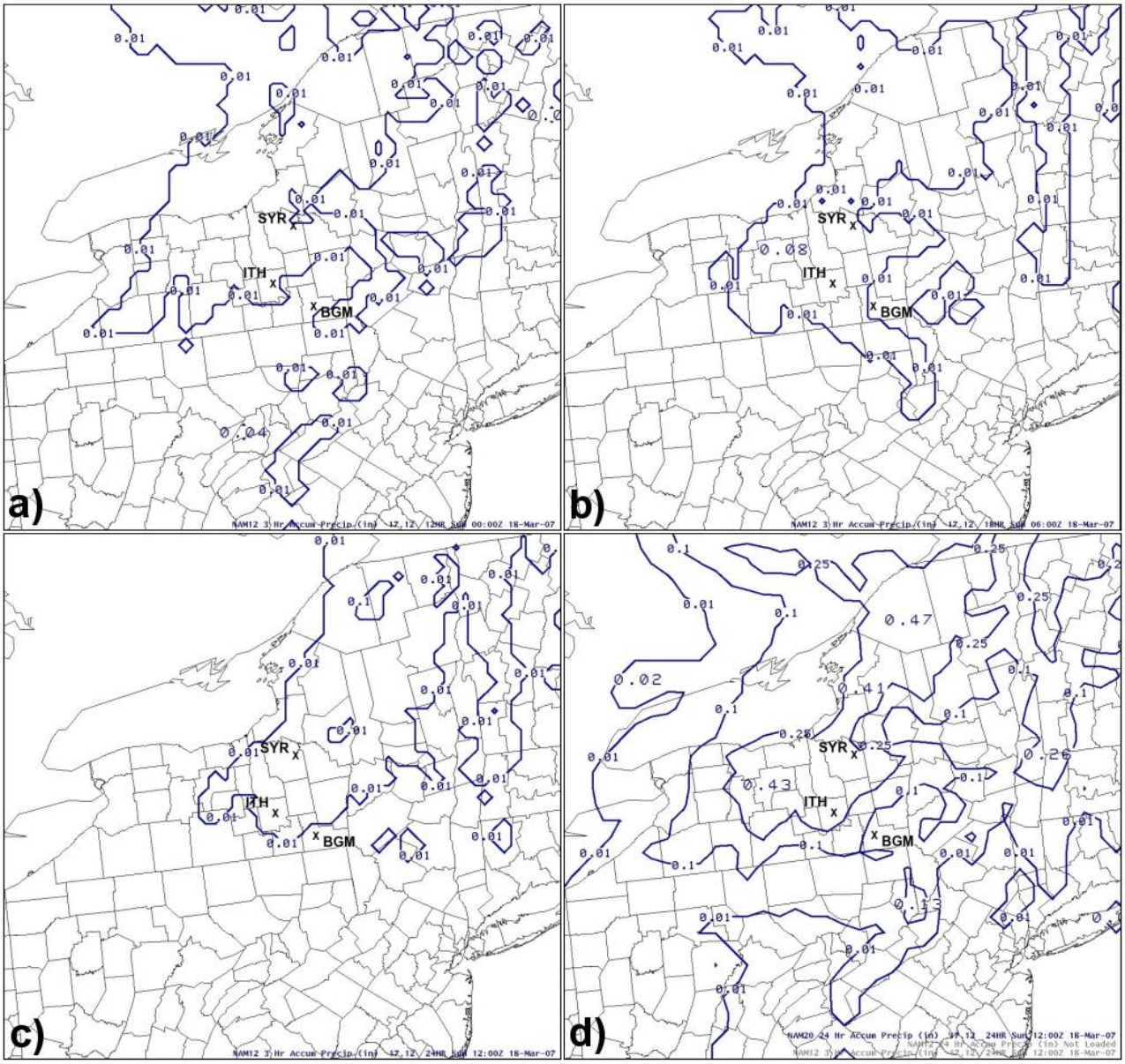

Fig. 16. 12 UTC 17 March 2007 NAM forecast 3-hour quantitative precipitation (inches) valid at a) 00 UTC 18 Mar. 2007, b) 06 UTC 18 Mar. 2007, c) 12 UTC 18 Mar. 2007; d) 12 UTC 17 March 2007 NAM 24-hour quantitative precipitation (inches) valid at 12 UTC 18 Mar. 2007.

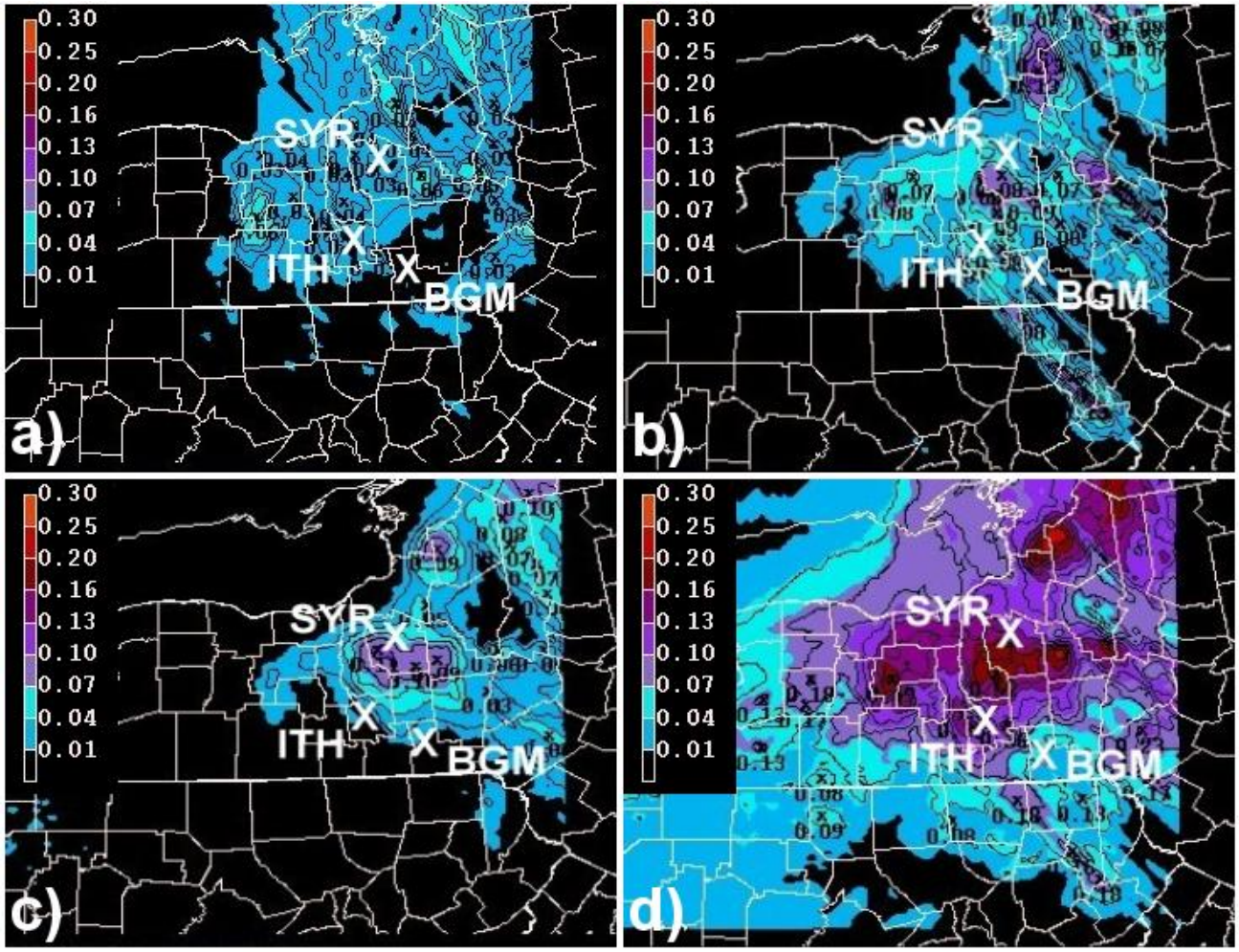

Fig. 17. 12 UTC 17 March 2007 6-km WRF 3 hour quantitative precipitation forecast (inches) valid at a) 00 UTC 18 Mar. 2007, b) 06 UTC 18 Mar. 2007, c) 12 UTC 18 Mar. 2007; d) 12 UTC 17 Mar. 2007 6 km WRF 24-hour quantitative precipitation forecast valid at 12 UTC 18 Mar. 2007.

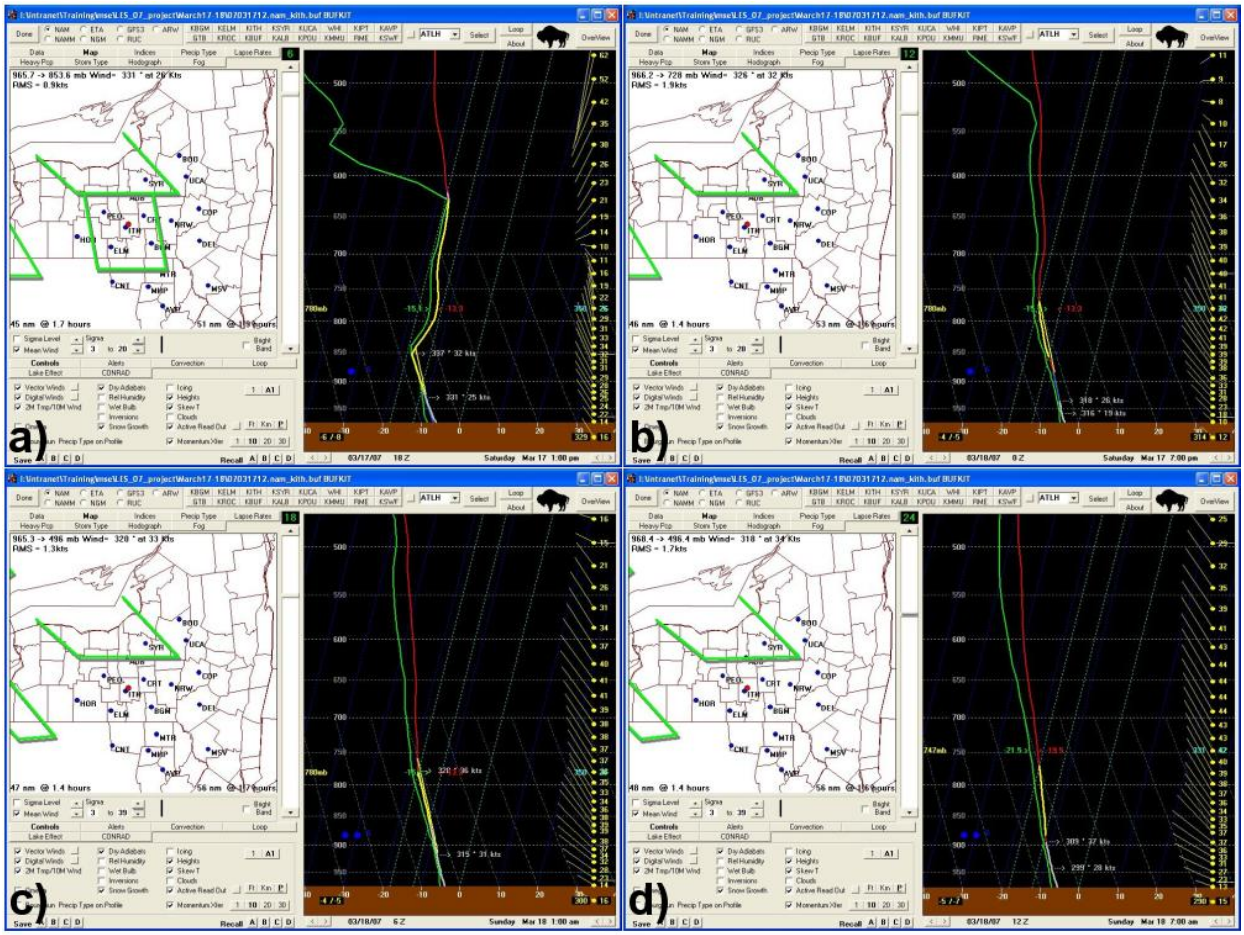

Fig. 18. 12 UTC 17 March 2007 NAM model forecast soundings valid at SYR as displayed by BUFKIT software and valid at a) 18 UTC 17 Mar. 2007, b) 00 UTC 18 Mar. 2007, c) 06 UTC 18 Mar. 2007, and d) 12 UTC 18 Mar. 2007.

LES Checklist Results	Similar Events for Site: ITH 1800 UTC					
Parameter	Your Values	Values 11/09/2004 at 1800 UTC	Values for 04/05/2004 at 0000 UTC	Values for 12/27/2005 at 0000 UTC	Values for 03/22/2004 at 0000 UTC	Values for 12/07/2003 at 1800 UTC
Mean Wind Direction:	331	331	329	324	322	337
Mean Wind Speed (knots):	26	12	36	32	32	29
850 mb Temperature (°C):	-16	-13	-10	-8	-14	-10
Lake - 850 mb Temperature Difference (°C):	18	21	13	12	17	15
Inversion Height (mb):	850	790	810	860	870	880
Moisture Depth (mb):	340	170	400	240	180	160
Dendritic Depth (mb):	270	40	180	0	120	0
Max Omega in the Dendritic Zone:	2	-1	-1	0	0	0
Max Tdd below 900 mb:	2	3	1	1	2	2
RMS Wind:	0.9	1.2	2.2	1.9	2	1.7
Persistent:	no	no	no	no	no	no
a)		Show 11/09/2004 at 1800 UTC	Show 04/05/2004 at 0000 UTC	Show 12/27/2005 at 0000 UTC	Show 03/22/2004 at 0000 UTC	Show 12/07/2003 at 1800 UTC

LES Checklist Results	Similar Events for Site: ITH 0000 UTC					
Parameter	Your Values	Values 01/26/2006 at 0000 UTC	Values for 04/05/2004 at 0000 UTC	Values for 01/17/2005 at 1800 UTC	Values for 03/03/2006 at 1800 UTC	Values for 12/27/2005 at 0000 UTC
Mean Wind Direction:	327	326	329	319	325	324
Mean Wind Speed (knots):	30	30	36	15	30	32
850 mb Temperature (°C):	-12	-11	-10	-20	-18	-8
Lake - 850 mb Temperature Difference (°C):	14	13	13	23	20	12
Inversion Height (mb):	500	500	810	750	850	860
Moisture Depth (mb):	450	270	400	250	110	240
Dendritic Depth (mb):	90	120	180	70	70	0
Max Omega in the Dendritic Zone:	-2	0	-1	-2	-4	0
Max Tdd below 900 mb:	1	1	1	2	3	1
RMS Wind:	1.9	1.5	2.2	1.6	1.6	1.9
Persistent:	yes	no	no	no	no	no
b)		Show 01/26/2006 at 0000 UTC	Show 04/05/2004 at 0000 UTC	Show 01/17/2005 at 1800 UTC	Show 03/03/2006 at 1800 UTC	Show 12/27/2005 at 0000 UTC

LES Checklist Results	Similar Events for Site: ITH 0600 UTC					
Parameter	Your Values	Values 03/04/2006 at 1200 UTC	Values for 03/04/2006 at 0600 UTC	Values for 01/26/2006 at 0600 UTC	Values for 12/08/2006 at 1200 UTC	Values for 02/27/2006 at 0600 UTC
Mean Wind Direction:	320	321	320	320	323	318
Mean Wind Speed (knots):	33	32	40	32	32	28
850 mb Temperature (°C):	-13	-11	-16	-13	-19	-21
Lake - 850 mb Temperature Difference (°C):	15	13	18	15	26	22
Inversion Height (mb):	500	880	850	880	770	800
Moisture Depth (mb):	330	170	220	190	250	140
Dendritic Depth (mb):	70	50	100	120	80	80
Max Omega in the Dendritic Zone:	-3	-1	-2	-3	-5	-3
Max Tdd below 900 mb:	1	3	2	2	2	2
RMS Wind:	1.3	2.2	2.6	1.9	1.8	1.8
Persistent:	yes	yes	yes	yes	no	yes
c)		Show 03/04/2006 at 1200 UTC	Show 03/04/2006 at 0600 UTC	Show 01/26/2006 at 0600 UTC	Show 12/08/2006 at 1200 UTC	Show 02/27/2006 at 0600 UTC

LES Checklist Results	Similar Events for Site: ITH 1200 UTC					
Parameter	Your Values	Values 03/19/2006 at 0600 UTC	Values for 01/25/2005 at 0600 UTC	Values for 01/20/2004 at 1200 UTC	Values for 12/14/2004 at 0600 UTC	Values for 11/09/2004 at 0600 UTC
Mean Wind Direction:	318	315	316	315	317	316
Mean Wind Speed (knots):	34	29	30	28	25	18
850 mb Temperature (°C):	-14	-16	-15	-14	-12	-11
Lake - 850 mb Temperature Difference (°C):	16	19	18	17	17	19
Inversion Height (mb):	500	820	810	880	850	700
Moisture Depth (mb):	330	190	200	200	200	280
Dendritic Depth (mb):	110	130	100	170	0	80
Max Omega in the Dendritic Zone:	-1	-2	-1	0	0	-3
Max Tdd below 900 mb:	1	2	2	3	1	2
RMS Wind:	1.7	1.8	1.9	1.7	1.4	2.2
Persistent:	no	no	no	no	no	no
d)		Show 03/19/2006 at 0600 UTC	Show 01/25/2005 at 0600 UTC	Show 01/20/2004 at 1200 UTC	Show 12/14/2004 at 0600 UTC	Show 11/09/2004 at 0600 UTC

Fig. 19. Tabular output from the WFO BGM pattern recognition application for forecasts valid at a) 18 UTC 17 Mar. 2007 b) 00 UTC 18 Mar. 2007, c) 06 UTC 18 Mar. 2007, and d) 12 UTC 18 Mar. 2007.

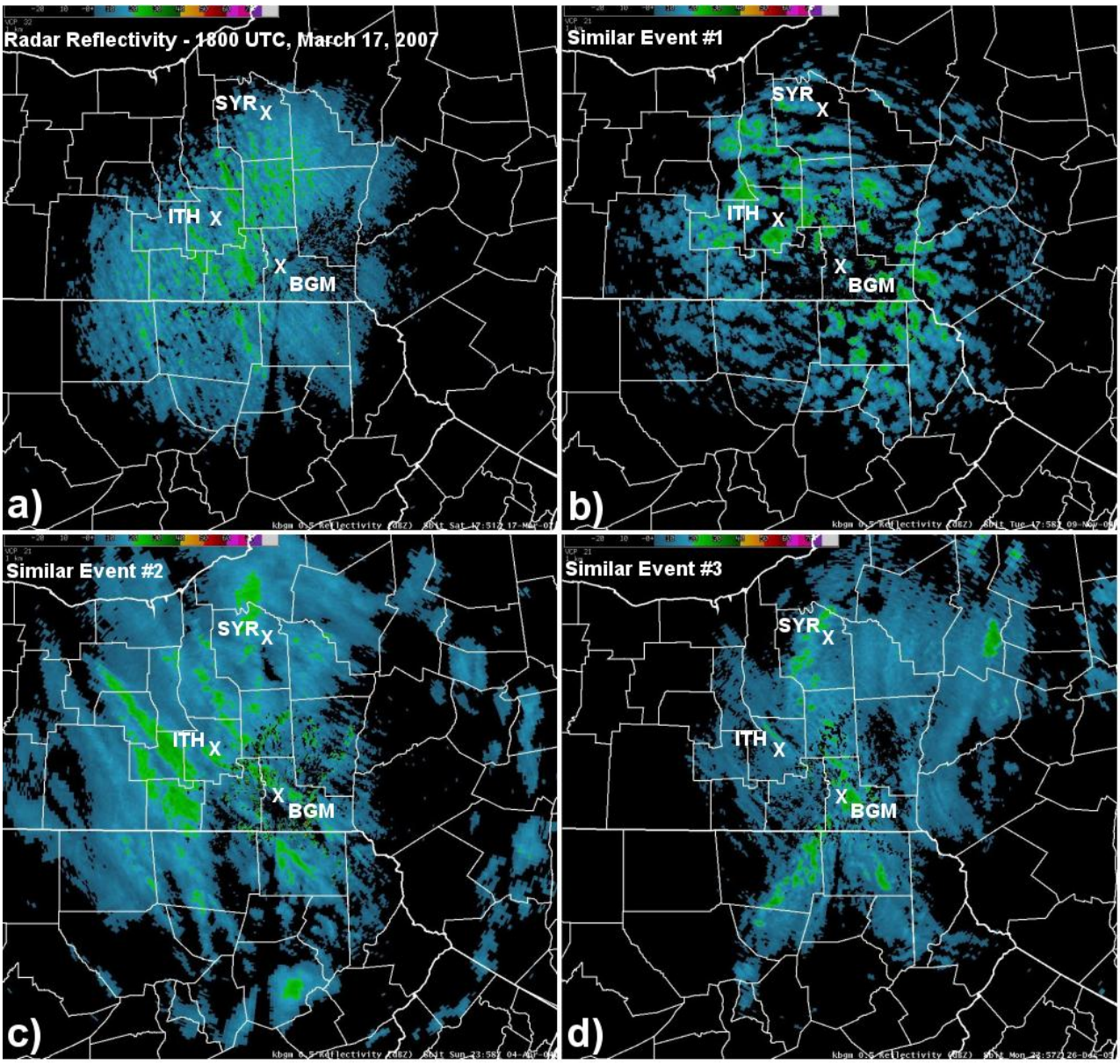

Fig. 20. (a) Observed 0.5º radar reflectivity from the case study at 18 UTC 17 March 2007; (b-d) Imagery from 3 corresponding similar events selected by the pattern recognition application.

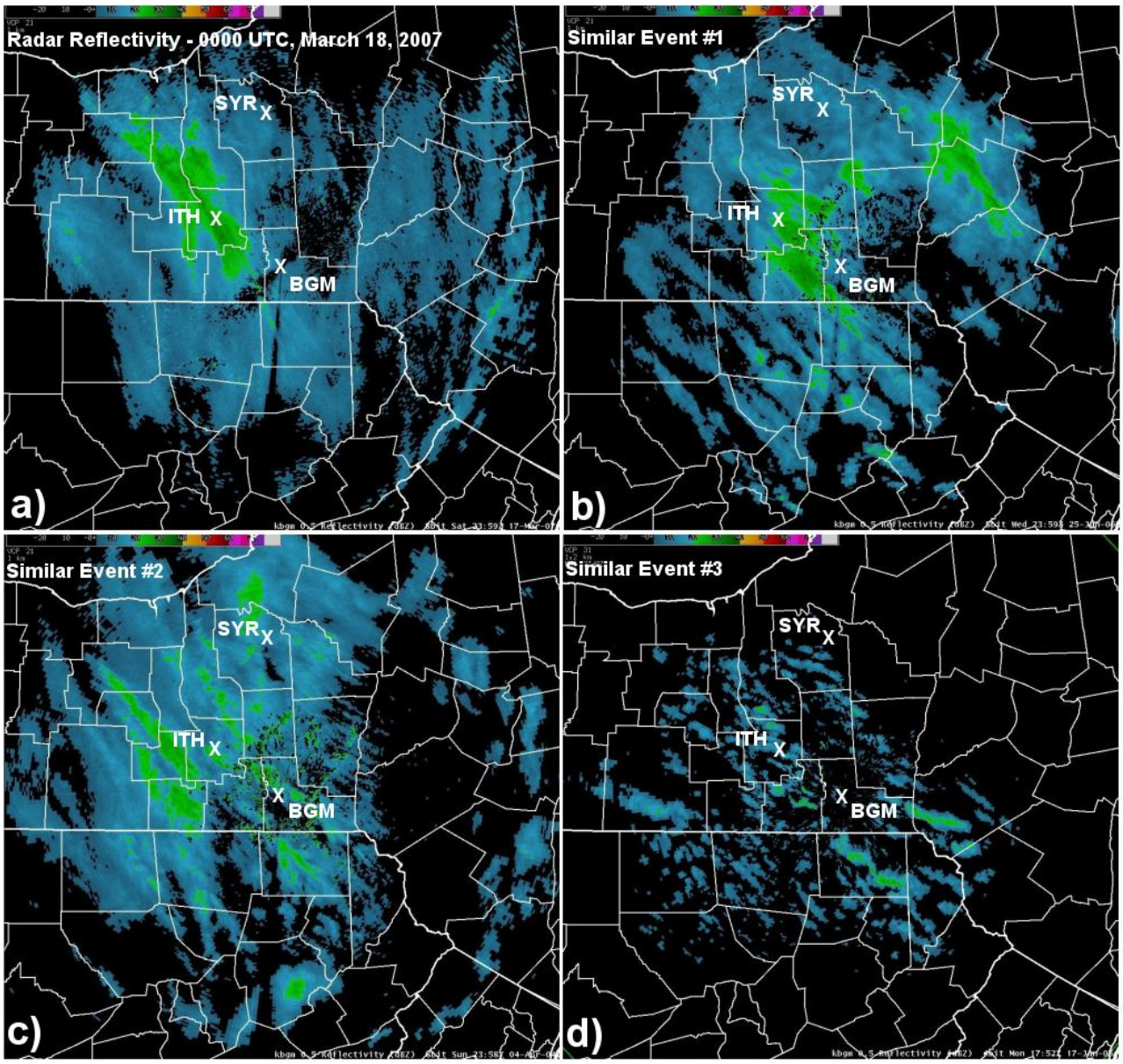

Fig. 21. (a) Observed 0.5º radar reflectivity from the case study at 00 UTC 18 March 2007. (b-d) Imagery from 3 corresponding similar events selected by the pattern recognition application.

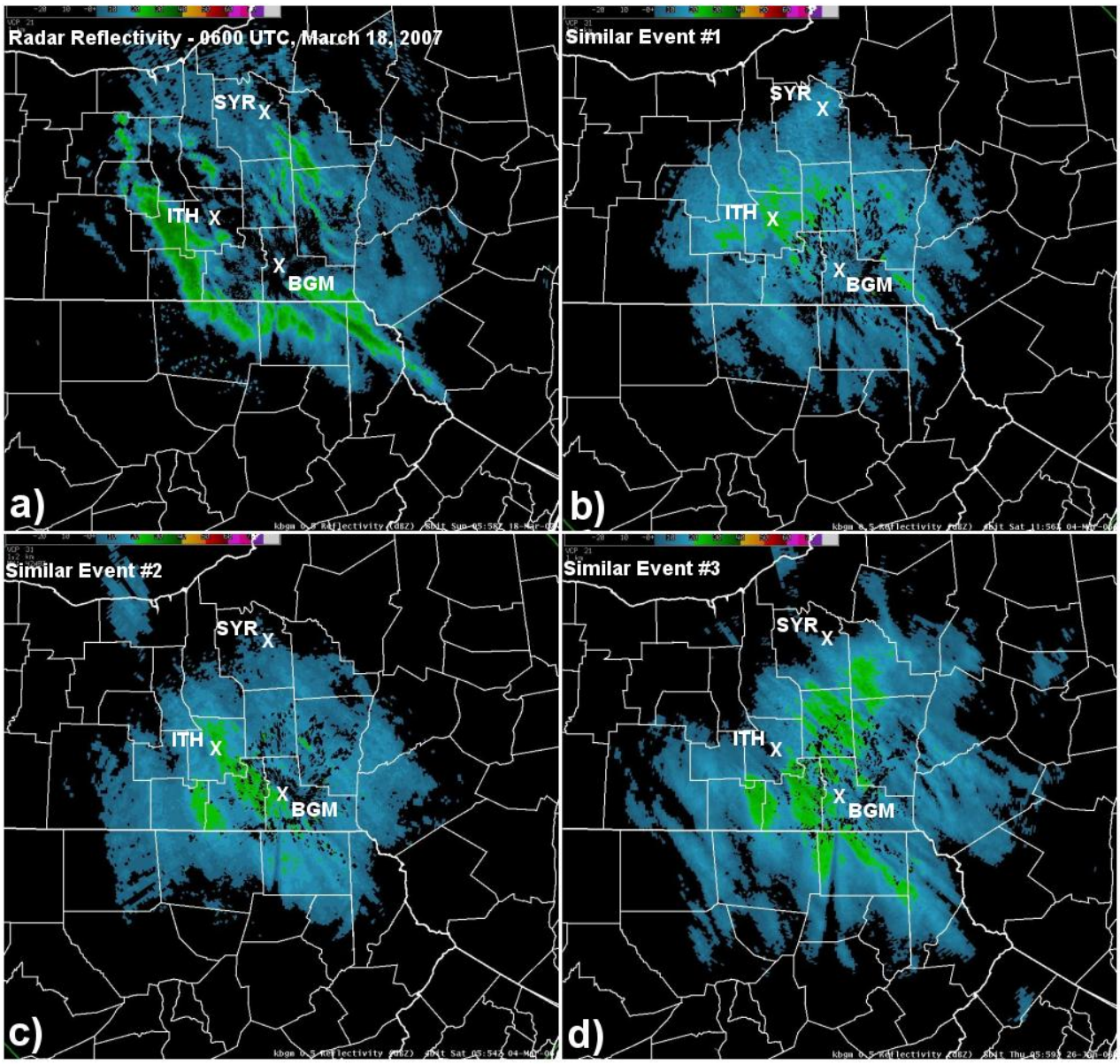

Fig. 22. (a) Observed 0.5º radar reflectivity from the case study at 06 UTC 18 March 18 2007; (b-d) Imagery from 3 corresponding similar events selected by the pattern recognition application.

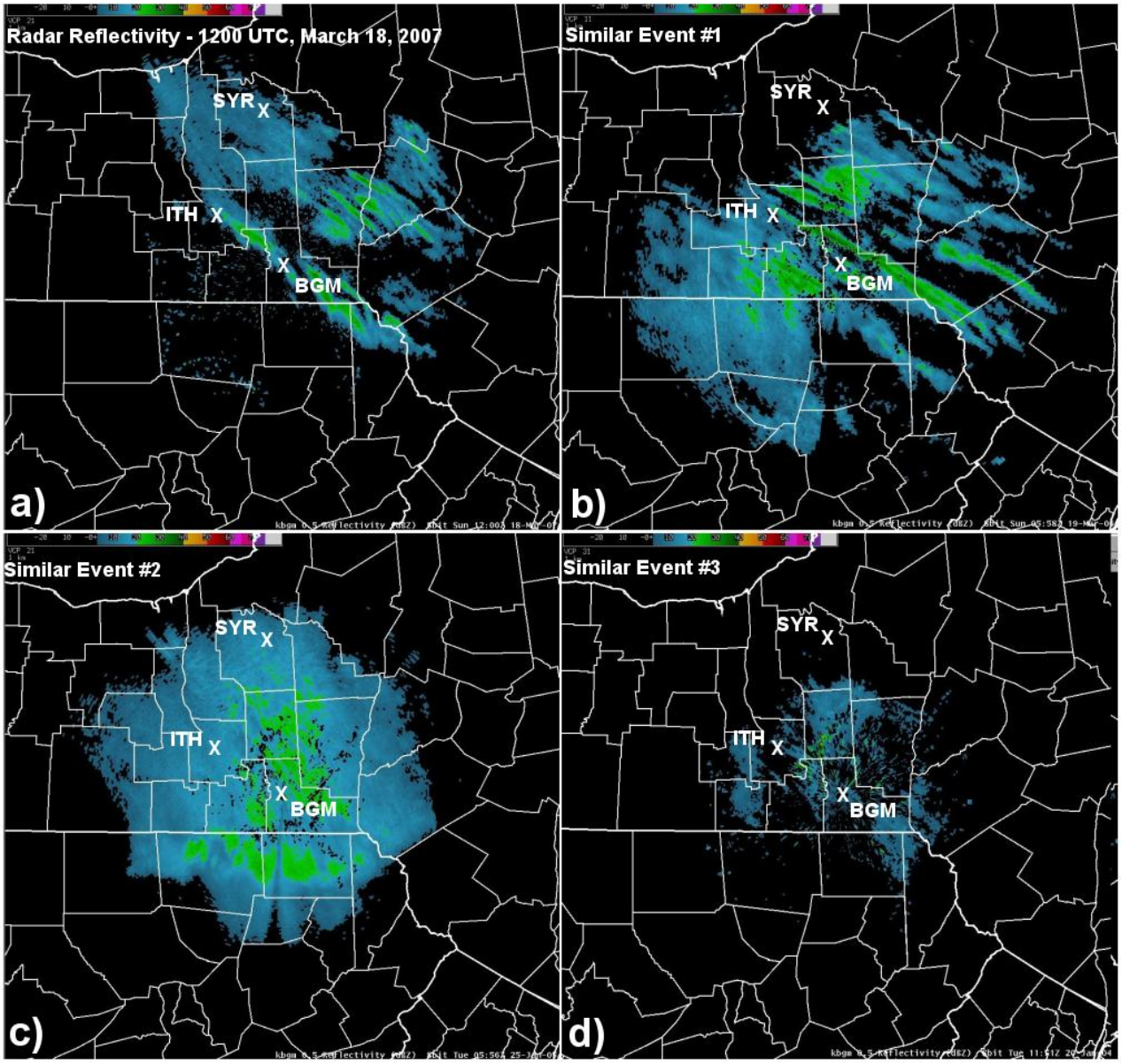

Fig. 23. (a) Observed 0.5º radar reflectivity from the case study at 12 UTC 18 March 2007. (b-d) Imagery from 3 corresponding similar events selected by the pattern recognition application.

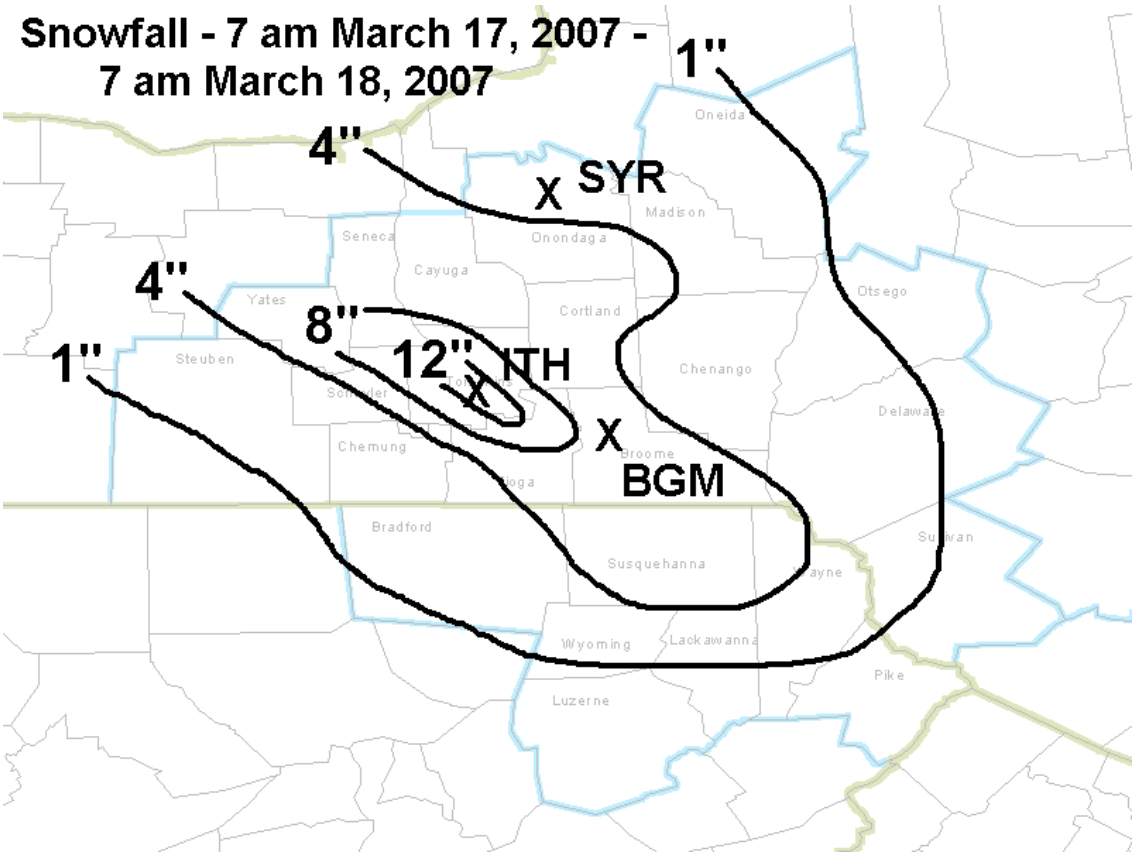

Fig. 24. Observed snowfall from 12 UTC 17 March 2007 through 12 UTC 18 March 18 2007.